MAY. - AUG. 2001
Volume VII Number II
ISSN 0859 144X

THE ASEAN JOURNAL OF RADIOLOGY

Published by The Radiological Society and
The Royal College of Radiologists of Thailand,
Bangkok, Thailand

Started through an educational grant from Bracco since 1995

TOSHIBA

GLOBAL IMAGING •MEDICAL SYSTEMS

Medical Equipment and Systems

Since the development of our X-ray tube in 1914,Toshiba Medical Systems Company has grown into one of the world's leading diagnostic imaging manufacturers, contributing to the advancement of medicine. Our operations include Research & Development, design, production, sales, services and support of diagnostic imaging equipment and systems. These and other activities have won the highest praise in the global medical market. The trust of our customers is a major factors in charting our course towards a new future in medicine.

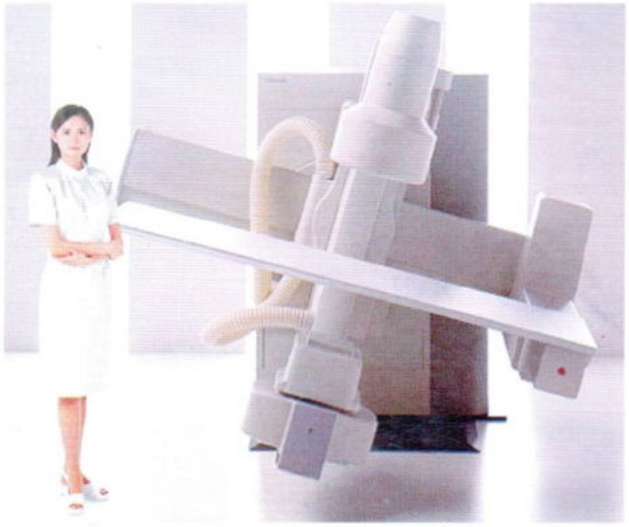

Multipurpose X-ray System : Model ULTIMAX

Toshiba's vision is to provide solutions to the medical professionals that help save patients' lives while offering reliable products with a long service life.

MRI Scanner : Model Excelart

Multislice CT Scanner : Model Aquilion MULTI

Whether the most appropriate solution is a single product or a complex combination of multiple modalities and imaging networks, Toshiba's philosophy is to be a long-term reliable partner with our customers.

That's why we say " Toshiba, Made for Life "

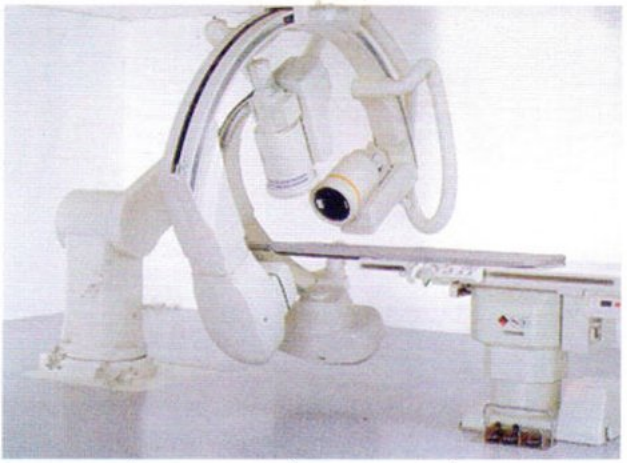

Biplane Angiography System : Infinix CB

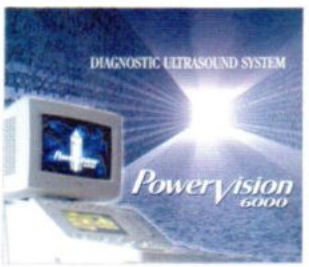

Powervision 6000

Made for Life

(SOLE DISTRIBUTOR)

CMC BIOTECH CO., LTD.
364 Muban Town-in-Town, Soi Ladphrao 94, Ladphrao Road, Wangthonglang, Bangkok 10310
Tel. 66(0) 2530-4995 (automatic 8 lines) Fax: 66(0) 2539-6903
Northern Branch (Chiangmai) Tel. 66(0) 5328-3261 Fax. 66(0) 5320-4463 Mobile Phone (01) 445-3766
North Eastern Branch (Khon Kaen) Tel. 66(0) 4334-1642 Fax. 66(0) 4334-1643 Mobile Phone (01) 431-3385
Southern Branch (Songkhla) Tel. 66(0) 7442-9803 Fax. 66(0) 7442-9804 Mobile Phone (01) 573-4937

MAY. - AUG. 2001
Volume VII Number II

ISSN 0859 144X

THE ASEAN JOURNAL OF RADIOLOGY

**Published by The Radiological Society and
The Royal College of Radiologists of Thailand,
Bangkok, Thailand**

Started through an educational grant from Bracco since 1995

Chief Editor

Professor Kawee Tungsubutra
Kaweevej Hospital, 318 Taksin Road, Dhonburi, Bangkok 10600, Thailand.

Asean Journal of Radiology.
Instructions for Authors.

1. The Asean Journal of Radiology publishes the papers on Radiological Sciences, such as research work, review articles, case reports, innovations in Medical Sciences related to all branches of Radiology, and letters to the editor. The aforementioned materials can be written in English only.

2. The authors have to submit 2 copies of the manuscript and a diskette: **to Prof. Dr. Kawee Tungsubutra.** 318 Kaweevej Hospital, Taksin Road, Dhonburi, Bangkok 10600, Thailand.

3. The original copy to be submitted must be typed in a double space on one side of the page of 8.1/2" x 11.1/2" paper.

4. The format of the article must include :

a. Title page and address of the author (s)
b. Abstract
c. Introduction (Background)
d. Material and Method
e. Results and discussion (Tables and Illustrations)
f. Acknowledgement (if any)
g. References (Follow the Vancouver style developed by ICMJE)

5. We will provide 10 copies of reprints for the author (s) who submit (s) an article for publication in the Asean Journal.

6. The illustrations and tables must be clearly prepared with legends in English as they are the art works to be reproduced.

7. The authors are reponsible for the contents of the article as to its facts and findings.

8. Ethics.

Paper reporting studies which might be interpreted as human experimentation (e.g. controlled trials) should conform to the standards of the Declaration of Helsinki (see British Medical Journal 1964:2:177) and should indicate that, approval that such studies may proceed, has been granted by the local or hospital Ethics Committee.

When reporting experiments on animals indicate whether the institution's or the National Research Council's guide for, or any national law on, the care and use of laboratory animals was followed.

BRACCO EDUCATION

Asia - Oceania

Asian-Oceanian Seminars on Diagnostic and Interventional Radiology 2001

Neuroradiology and Head & Neck Radiology: The Impact of Neuroimaging and Intervention in the 21st Century

June 2 - 3
Sapporo, Japan
Programme Leader:
Prof K Miyasaka

Neuroradiology

Oct 4 - 5
Bali, Indonesia
Programme Leaders:
Dr Zulkarnain Sjair
Dr Prijo Sidipratomo

For further information please contact:

ASDIR Secretariat
Huntington Consultancy Pte Ltd
47 Hill Street #06-04
S.C.C.C.I. Building
Singapore 179365
Tel: +65-339 2883
Fax: +65-339 2272
E-mail: asdir.secretariat@huntington.com.sg

BRACCO
THE IMAGE OF INNOVATION

www.bracco.com/imaging

Bracco research presents
the new nonionic contrast medium

iomeron®

iomeprol

The multifactorial solution

BRACCO
THE IMAGE OF INNOVATION

http://www.bracco.com/imaging

THE ASEAN JOURNAL OF RADIOLOGY

Volume VII Number II MAY. - AUG. 2001

CONTENTS

THE ASEAN JOURNAL OF RADIOLOGY

Volume VII Number II MAY. - AUG. 2001

CONTENTS

ADRENOCORTICAL CARCINOMA IN INFANT WITH IVC EXTENSION

Laddawan VAJRAGUPTA M.D.[1]
Tanya JEERASOMBOONYING M.D.[1]
Suttipong WACHARASINDHU M.D.[2]

ABSTRACT

Primary adrenocortical carcinoma is a relatively rare malignancy in infancy and childhood. It is a highly malignant and locally invasive tumor. Local extension can occur by vascular and visceral invasion. There has been a few isolated cases of adrenocortical carcinoma with vena caval involvement in infancy and childhood. We report one case of a 10 month- old infant of an adrenocortical carcinoma with vena caval involvement. The diagnosis is depicted by ultrasonography, computed tomography and pathologic correlation.

INTRODUCTION

Adrenocortical carcinoma is a relatively rare neoplasm in infancy and childhood, accounting for less than 0.2% of all pediatric cancer.[1,2] The annual incidence has been calculated as three per million in children under 20 years.[1] Seventy five percent of children who develop adrenocortical carcinoma are less than 5 years old at diagnosis[3]. The median age at diagnosis is 4.3 years (3days-15.8 years). The tumor is more common in girl. Greater than 75% of adrenocortical carcinomas are functional, secreting one or more hormones (androgen, cortisol, aldosterone or estrogen).[3] It is a highly malignant tumor which tends to make a rapid extension locally by vascular and visceral invasion with distant metastasis to lung, bone and brain. Inferior vena caval invasion can occur in 25- 35% of cases[4] but there has been a few isolated cases of adrenocortical carcinoma with vena caval involvement in infancy and childhood. One case of childhood adrenocortical carcinoma of right adrenal gland with IVC extension diagnosed by venography was reported in 1983[5] and three cases of childhood adrenocortical carcinoma with extension into IVC and right atrium diagnosed by ultrasound, CT and MRI were reported in 1990.[6] We report a 10-month-old infant boy of adrenocortical carcinoma with vena caval involvement depicted by ultrasound and CT scan.

CASE REPORT

A 10 month-old infant boy presented in1998 with a 4-month history of rapid gaining of weight. Examination revealed Cushinoid features, facial acne, hirsutism, hypertrophy of penis and mild pubic hair (Fig.1). The patient had moderate to severe hypertension. Bone age was normal. No abdominal mass was palpable.

Cushing's syndrome was diagnosed on the basis of an elevated mean serum cortisol with lack of cortisol circadian rhythm and absence of suppression on LDST. The 24-hour urinary ketosteriod was increased.

[1] Department of Radiology, Faculty of Medicine, Chulalongkorn University, Bangkok, Thailand.
[2] Department of Pediatric, Faculty of Medicine, Chulalongkorn University, Bangkok, Thailand.

Ultrasound examination showed a 3.6x3.2 centimeter inhomogeneous hypoechoic mass at the left adrenal region. Evidence of the internal echo in IVC and left renal vein represent tumor thrombus was noted (Fig.2).

Abdominal CT showed a 4 centimeter well-defined rounded soft tissue density mass in the left adrenal region with homogeneously enhancement. Evidence of dilated left adrenal vein, containing thrombus and also thrombus in left renal vein and IVC were demonstrated (Fig.3). The contralateral adrenal gland appeared normal. The left renal stone was seen (Fig.4). There are abundant of subcutaneous fat of the whole body.

At surgery, the left adrenal gland contained a 3.4 cm.-sized, well- circumscribed tumor with thrombus in the left adrenal vein (Fig.5). Left adrenalectomy and tumor thrombus removal were performed. Histologically, the tumor consisted of nets of round cells containing vesicular nuclei and small nucleoli which compressed the normal structure. Evidence of moderate nuclear pleomorphism, abnormal mitosis, tumor necrosis and capsular invasion were demonstrated. The diagnosis was that of adrenocortical carcinoma. The patient died on day 20th after operation due to sepsis and adrenal insufficiency.

Fig. 1. A 10 month-old infant boy with Cushinoid features.

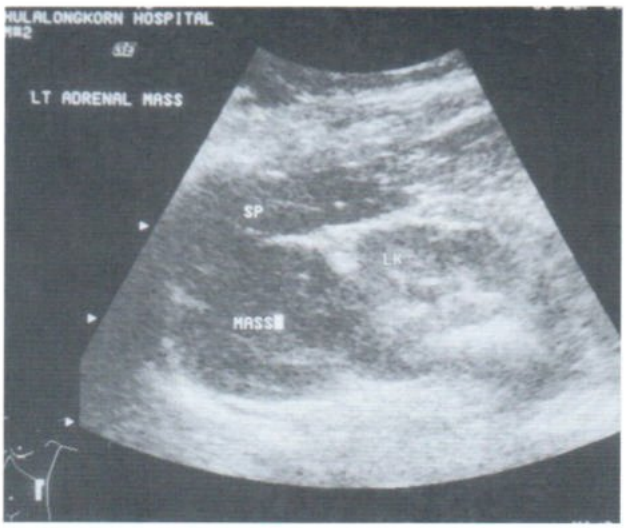

2A

Fig. 2A. Longitudinal subcostal sonogram of left upper quadrant demonstrates a 3 cm. inhomogeneous hypoechoic mass at the left adrenal region. (LK = left kidney, SP = spleen)

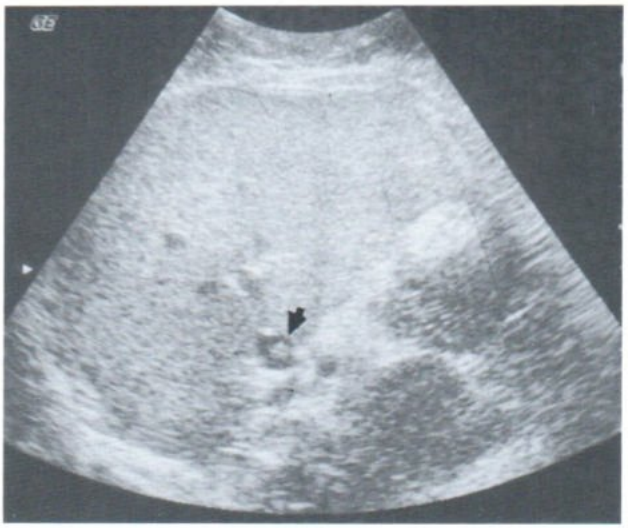

2B

Fig. 2B. Transverse sonogram shows intraluminal echogenic thrombus within IVC (arrowhead).

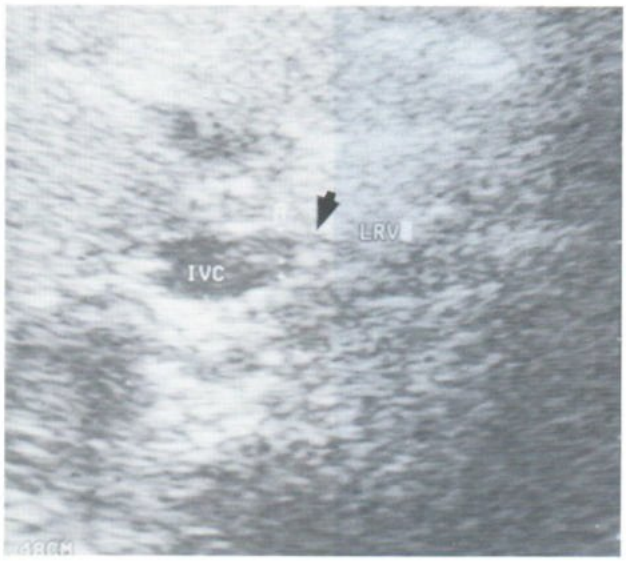

2C

Fig. 2C. Transverse sonogram shows echogenic thrombus in left renal vein (arrowhead). (IVC = inferior vena cava, LRV = left renal vein)

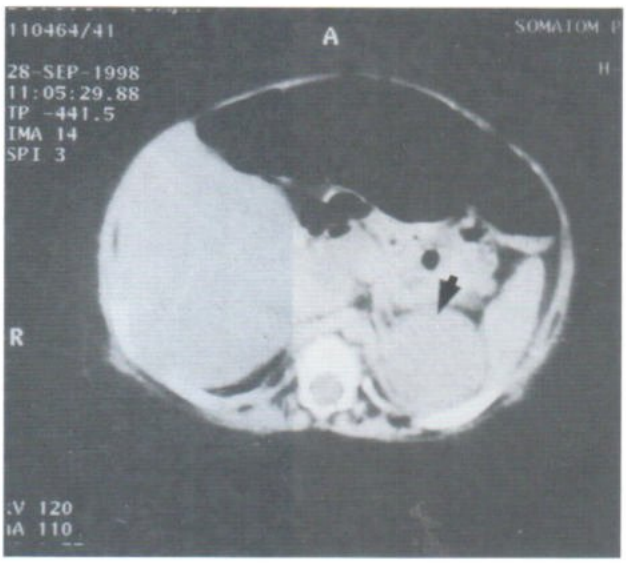

3A

Fig. 3A. Unenhanced CT scan shows a well-defined rounded left adrenal soft tissue density mass (arrowhead).

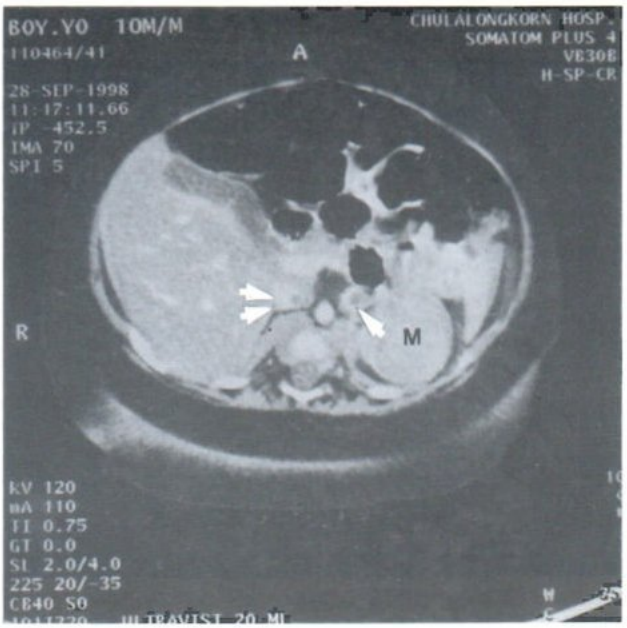

3B

Fig. 3B. Enhanced CT scan shows homogeneous enhancement of the left adrenal mass (m). Dilated left adrenal vein, containing thrombus. (arrow head). Thrombus in IVC (double arrowheads).

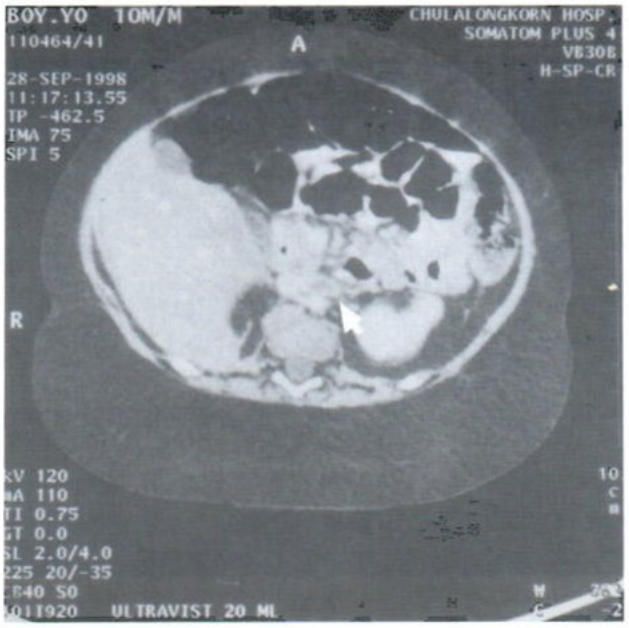

3C

Fig.3C. Enhanced CT scan shows thrombus in left renal vein (arrowhead).

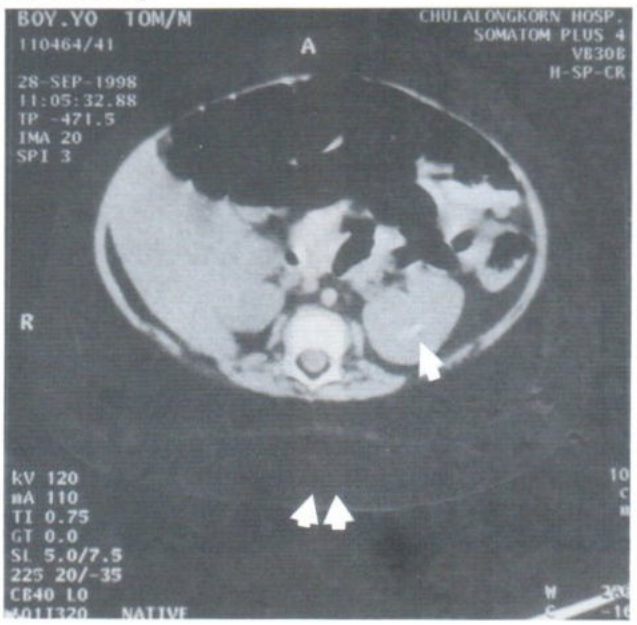

Fig. 4. Unenhanced CT scan shows stone in the left kidney (arrowhead). Abundant of subcutaneous fat (double arrowheads).

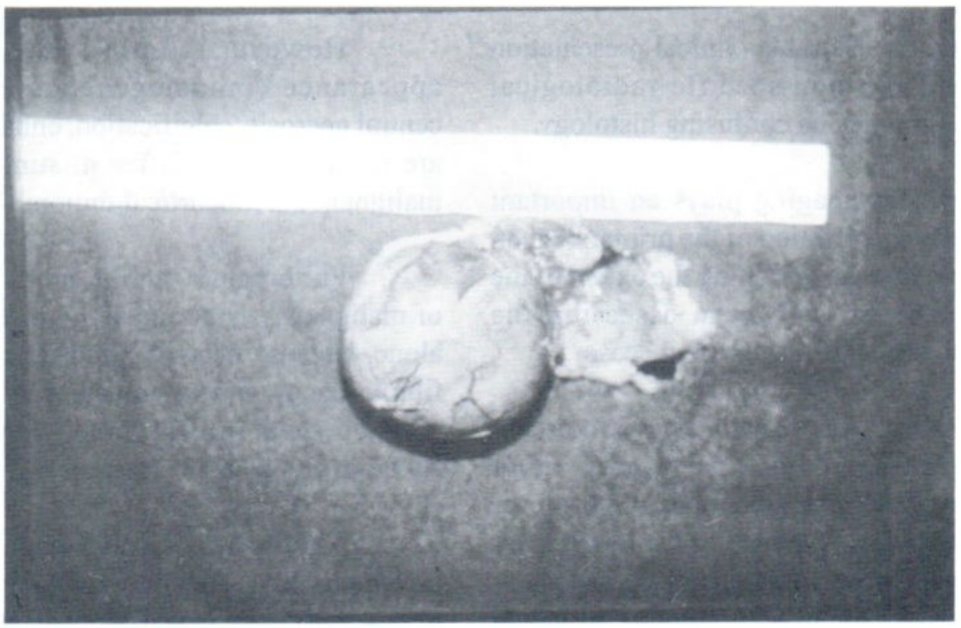

Fig. 5. Gross specimen, removed at surgery, was an adrenocortical carcinoma.

DISCUSSION

Primary adrenocortical carcinoma is a rare malignancy in infancy and childhood. Although childhood adrenocortical carcinoma extremely uncommon, it is still the most common tumor occurring in the adrenal cortex.[7] It is much less common than neuroblastoma but slightly more common than pheochromocytoma. Most pediatric patients with adrenocortical carcinoma have hormonally active tumors. The most common manifestation being either virilism or a mixture of virilism and Cushing's syndrome.[2] Adrenocortical carcinoma with cortisol production is the most common cause of Cushing's disease in children. Cushing's syndrome refers to the manifestation of glucocorticoid excess and it is a presenting symptom in our patient. On CT scan, evidence of left renal calculi was detected in our patient. The renal calculi occur approximately 15% of the patients of Cushing's syndrome, and renal colic may occasionally be a presenting complaint.[7] These calculi are a consequence of glucocorticoid-induced hypercalciuria. Serum calcium and phosphorus concentrations are normal; however hypercalciuria occur in 40% of these patients.

The diagnosis of the non-functioning tumor is often delayed until the mass become huge or systemic symptoms arise. Adrenocortical carcinoma has been found to be associated with Beckwith-Wiedemann syndrome, hemihypertrophy and Li-Fraumeni syndrome.[1]

It is a highly malignant and locally invasive tumor. Extensive local tumor invasion being present in just over 50% of the carcinomas in the present series[5]. Distant metastasis to lungs, bone and brain occurs in many cases. Inferior vena caval, adrenal vein or renal vein invasion are found in 25 to 35% of cases.[4] Extension into the right atrium may be found.[6]

Adrenocortical carcinoma in childhood may be a considerable diagnostic problem by

virture of its rarity, variable clinical presentation and biochemistry, non-specific radiological findings and, at times its confusing histology.

Diagnostic imaging plays an important role in the early localization of the primary lesion of the adrenal gland and defining the extent of the primary tumor as well as in assessing the presence or absence of metastatic disease.

Sonography can usually reveal the separation between the adrenal mass and a tumor arising in the liver or the upper pole of the kidney by characteristic displacement of the retroperitoneal fat planes. Sonographic appearance of pheochromocytoma, adrenal adenoma or carcinoma may be similar. While still small, most lesions present with a homogeneous echo pattern that usually becomes complex as the lesion grow, reflecting areas of necrosis or hemorrhage.[9]

On sonography the primary tumor of adrenocortical carcinomas are usually large and the complex echo pattern correlates with the central necrosis, hemorrhage and calcification. Radiating septa or an echogenic, capsule-like rim can be seen. Occasionally the entire mass may be either hypoechoic or hyperechoic.[9] Color Doppler imaging is a non-invasive method to evaluate vascular extension of tumor, especially in acute thrombosis. It is particularly effective in demonstrating a partially patent lumen when standard gray scale examination suggests total occlusion. Intrinsic obstruction of the IVC related to thrombosis can be either partial or complete.[10]

The CT appearance of adrenocortical carcinoma is non-specific. It may be heterogeneous with inhomogeneous contrast enhancement. In our patient, the sonographic appearance of the primary tumor showed an inhomogeneous hypoechoic mass and abdominal CT scan revealed homogeneously enhanced soft tissue mass.

However criteria related to size and appearance (inhomogeneous enhancement, central necrosis, calcification, enhancing capsule) are not reliable in differentiating benign from malignant adrenocortical tumors.

Furthermore, unlike adults, the diagnosis of malignancy is not made by histologic criteria alone, because necrosis, nuclear pleomorphism, fibrous bands, and vascular and capsular invasion may be seen in childhood adrenal cortical adenomas as well as carcinomas.

Although differential diagnosis of adrenal carcinoma from adenoma may be difficult, MRI plays a role in the differentiation between malignant tumor and adenoma. More recently, chemical shift MR imaging technique has been used to detect lipid within an adrenal mass. Because significant amount of lipid often present in adrenal adenomas and typically absent in most metastases and other nonadenomatous adrenal masses. Using breathhold opposed- phase gradient echo imaging, Mitchell et al showed a relative loss of signal intensity of adrenal masses in 95% of adenomas and in none of their nonadenomas.[12]

IVC extension can occur at four different levels[4] : level 1, tumor thrombus occurring only at the entry of the renal vein (left-sided tumors); level 2, tumor thrombus extending up to the IVC but remaining below the entry of the most inferior hepatic vein; level 3, refers to tumor thrombus extending into intrahepatic vena cava but below the diaphragm; and level 4, refers to tumor thrombus extending above the diaphragm or into the right atrium. All these four levels of IVC tumor thrombus require different surgical approaches. Therefore, when tumor thrombus is found, the exact extent, that is infrahepatic, intrahepatic, suprahepatic, or supradiaphragmatic, must be identified.

If the tumor thrombus is infrahepatic, the cardiothoracic bypass is usually unnecessary, and the tumor thrombus can be directly extracted from the vena cava after obtaining local control of the vena cava. Cardiothoracic by pass is the preferred method for the tumor thrombus at any of the other levels.

CT scan is the accented standard for evaluation of the primary tumor and involvement of the structures. Both CT scan and ultrasound are helpful in evaluating involvement of adrenal, renal and vena caval structure. MRI scanning can add to the precision of the evaluation because of the ability to display images of the IVC in coronal, sagittal and axial planes.

In our patient, evidence of tumor thrombus was demonstrated in left renal vein and infrahepatic IVC by both ultrasound and CT scan. The tumor thrombus in left adrenal vein was seen on CT scan.

Surgery is the main stay of treatment, since no effective adjuvant treatment is available. The prognosis is poor as most tumors which are locally invasive or having distant metastases at the time of presentation.

In conclusion, adrenocortical carcinoma is rare but is a highly malignant neoplasm in infancy and childhood. Local invasion with visceral and vascular involvement and distant metastases are common. Accurate preoperative assessment of local extension and IVC invasion is helpful in preparing for the surgical extirpation.

REFERENCES

1. S.K. Mayer, L.L., et al. Childhood adrenocortical tumors; Case series and reevaluation of prognosis. Journal of Pediatric Surgery 1997;32:911-915
2. G.S. Jones K.J. SHAH and J.R. Mann. Adrenocortical carcinoma in infancy and childhood ; A radiological report of 10 cases. Clinical Radiology 1985;
3. M.D., FACR. Adrenal neoplasms in children. Pediatric oncology imaging. Radiologic Clinics of North America 1997;35:1445-1448
4. Marc H. Siegelbaum, M.D., James E. Moulsdale, M.D., et al. Use of magnetic rasonance imaging scanning in adrenocortical carcinoma with vena caval involvement. Urology June 1994;43:869- 873
5. A. Daneman, Helen S.L. Chan and J. Martin : Adrenal carcinoma and adenoma in children ; A review of 17 patients. Pediatric Radiology 1983;13:11- 17
6. L.B. Godine, W.E. Berdon, R.C. Brasch and J.C.Leoniads. Adrenocortical carcinomas with extension into inferior vena cava and right atrium ; Report of 3 cases in children. Pediatric radiology 1990;20:166-168
7. Philip Felig, John D. Baxter, Lawrence A. Frohman. The adrenal cortex. Endrocrinology and Metabolism 1995;667
8. Sjirk J. Westra, M.D., Alejandra C. Zaninovic, M.D., Theodore R. Hall, M.D., Hooshang Kangaroo, M.D., M. Ines Boechat, M.D. Imaging of the adrenal gland in children. Radiographics 1994; 14:1328
9. A. Prando, S. Wallace, et al. Sonographic findings of adrenal cortical carcinomas in children. Pediatric Radiology 1990;20: 163- 165

10. Carol M. Rumack, M.D., Stephanie R. Wilson, M.D., J. William Charbonean, M.D. Diagnostic Ultrasound 1991:348
11. Hawkins EP, Cagle PT. Adrenocortical neoplasms in children. Am J Clin Pathol 1992;98:383
12. Melvyn Korobkin, M.D., and Isaac R. Francis, M.D. Imaging of adrenal masses. Urorogic Clinics of North America August 1997;24:608.

ROLE OF CONTRAST MR MAMMOGRAPHY IN THE INDETERMINATED BREAST DISEASES

Darunee BOONJUNWETWAT, M.D.[1] Saowanee SRIRATTANAPONG, M.D.[1]
Pichet SAMPATANUKUL, M.D.[2] Kris CHATAMRA, M.D.[3]

ABSTRACT

The purpose of this study is to evaluate the diagnostic capability of contrast MR mammography (MRM) in the problem of breast lesions that were indeterminated on mammography and ultrasonography.

The contrast MRM of twenty - two proven breast lesions was retrospectively reviewed. All lesions were indeterminated on mammography and sonography. There were eight cases received conserving breast treatment for carcinoma. The contrast MRM was performed by GE Signa 1.5 Tesla system. Only nine cases had post contrast dynamic study with signal time curve. All lesions were read and concensus by two radiologists using the same criteria based on MR morphologic features, patterns of enhancement and signal time curve. The qualitative and quantitative studies were integrated into the five points confidence scale (MRI score). The lesions were graded benign or malignant according to the MRI score (1,2 = benign and 3,4,5 = malignant). Furthermore, we analyzed the data of these lesions into two groups, group 1 without signal time curve and group 2 with signal time curve.

Twenty - two lesions were interpreted by using the MRI score, seven lesions were considered to be malignant and fifteen lesions were considered to be benign. The sensitivity, specificity, and accuracy in the diagnosis of breast disease were 75%, 92.8%, and 86.4% respectively. In comparison between the group 1 and group 2, the sensitivity, specificity, and accuracy in diagnosis were 60.0%, 80.0%, 70.0% in group 1 and 100%, 100%, 100% in group 2, respectively.

Contrast MRM is the effective imaging method for evaluation of the breast lesions that mammography and sonography were indeter-minated. Supplement dynamic study with signal time curve should improve the capability and provide superiority in establishing the correct diagnosis.

[1] Department of Radiology, Faculty of Medicine, Chulalongkorn University, Bangkok, Thailand
[2] Department of Pathology, Faculty of Medicine, Chulalongkorn University, Bangkok,Thailand
[3] Department of Surgery, Faculty of Medicine, Chulalongkorn University, Bangkok, Thailand

INTRODUCTION

Since the sensitivity of mammographic detection of lesions is reduced in dense breasts, augmented breasts and post conserving breast therapy whereas MRI of the breasts is increasingly used in addition to conventional mammography and ultrasonography. It is used to help patients with inconclusive findings of conventional breast imaging and to diagnose primary and recurrent breast cancer.[1-9]

Although the sensitivity and specificity of MRI in the detection of breast cancer have been reported in various studies. The sensitivity and specificity depend not only on criteria of interpretation, MRI technique and patient selection but also on the experiences of the radiologist. MRI of the breasts has been used in King Chulalongkorn Memorial Hospital since 1994. At the early time of the study, we used the shoulder coil and body coil for breast imaging, by the end of 1997 the bilateral breast surface coils were available. The goal of our study is to evaluate the diagnostic capability of contrast MR mammography (MRM) in those patients with indeterminated lesions by mammography and ultrasonography.

MATERIALS AND METHODS

We retrospectively reviewed MRI records in our Hospital since December 1994 to August 1999. Twenty contrast enhanced MRI studies of the breasts with available medical records were included in the study. All cases had mammography and ultrasonography performed showing indeterminated lesions. Eight cases had a history of carcinoma of the breast received conserving breast treatment with problem of residual tumor or fibrosis. The patient's age varied between 26-72 years old (mean = 46.7 years). Nineteen cases were female and one case was male. One of the women had 3 MRI studies of the breasts, one for the left breast and two for the right breast at different times. The final diagnosis was established by means of fine needle aspiration cytology (FNAC), biopsy or follow up by physical examination and mammography.

MRI studies of the breasts were performed by GE Signa 1.5 tesla system using a variety of imaging parameters, all with gadolinium contrast enhancement. Imaging protocols consisted of axial and sagittal spin echo T1W, axial or sagittal fast spin echo T2W images with fat suppression technique or short T1 inversion recovery (STIR) images. Post contrast enhanced dynamic study was performed in only 9 cases at 0, 1, 2, 3, 5 and 7 minutes by using 3D gradient echo images (SPGR) as well as the imaging subtraction and signal-time curve. Ten cases had been imaged in supine position using shoulder coil, two cases in prone position using body coil and the remaining eight cases had been used bilateral breast surface coils.

All qualitative images and quantitative analyses were reviewed by two radiologists and consensus was obtained for the MRI features without knowing conventional mammographic, sonographic and pathological findings. The MRI features were evaluated using these following criteria.

1. Lesion configuration. It was classified as a mass or non-mass related to the enhanced pattern as segmental, linear, regional or patchy. Regional and patchy configurations were both suggestive of benign breast changes.

2. Shape and borders. An irregular or even a spiculated shape was suggestive of malignant lesion, where as a round or oval shape suggested a benign mass.

3. The lesions internal architecture. The homogeneity and low signal internal septations both were suggestive of benignity. If it showed heterogeneous or peripheral enhancement (rim enhancement), this was suggestive of malignancy.

4. The signal time curve pattern was classified according to their shape as type I which was steady enhancement; type II, plateau of signal intensity; or type III, washout of signal intensity as shown in figure 1. A type I was indicative of benign lesion, where as type III strongly suggestive of malignancy. A type II may be found both in benign and malignant lesions.

Finally, the quantitative and qualitative assessments were combined into an integrated evaluation of the individual lesion rated on five points confidence scale (MRI score).

1. Definitely benign when morphological features were rated benign with homogeneous enhancement or type I signal time curve or when a non-mass related patchy or regional enhancement was found.
2. Probably benign when morphological features were rated benign with type II signal time curve or single morphological feature was rated malignant with type 1 signal time curve.
3. Possible malignant when one or two morphological features were rated malignant with patchy enhancement or type II signal time curve.
4. Probably malignant when single morphological feature was rated malignant with heterogeneous or rim enhancement or type III signal time curve.
5. Definitely malignant when all morphological features were characteristic of malignant with rim enhancement or type III signal time curve.

The classification of the lesions to be benign (negative) or malignancy (positive) depended on the MRI score, as shown in table 1. For calculation of sensitivity and specificity outcomes, the MRI score of 3, 4 and 5 were considered positive for malignancy while the MRI score of 1 and 2 were negative or benign. According to twenty-two lesions, twelve lesions were evaluated using signal time curve and ten lesions without using signal time curve.

Table 1. MRI score and lesion classification.

MRI SCORE	LESION
1, 2	Benign
3, 4, 5	Malignant

RESULTS

Twenty-two lesions were identified on MRI studies. Seven lesions were considered malignancy and fifteen lesions were considered benign on the basis of MRI score. The MRI classification related with the final diagnosis was shown in table 2.

According to the seven lesions considered malignancy on MRM, three lesions showed rim enhancement (Fig. 1), four lesions showed heterogeneous enhancement (Fig. 2). Three of seven lesions had signal time curve which showed to be type 3 in two lesions and type 2 in one lesion (Fig. 3 A,B). Among these seven lesions, six lesions were histological proven to be invasive ductal carcinoma. There was one case that MRM showed spiculated irregular lesion in left breast with heterogeneous enhancement and was

misinterpreted without signal time curve as malignancy (MRI score 4), this case had involuted asymetrical breasts on mammography and increased radiotracer uptake at left subareolar region on Tc^{99m} sestamibi. Needle-guide biopsy was finally performed and cytology showed to be adenosis. No malignant lesion was found during the follow-up time of 59 months.

In fifteen lesions of twelve cases considered benign related to MRI score 1 and 2 with benign morphological features and type 1 signal time curve (Fig. 4 A,B). Microdochectomy was performed in two cases and histopathology turned out to be intraductal papilloma. Fine needle aspiration cytology (FNAC) was performed in three cases and no malignant cell was found. One patient had biopsy, proved to be adenocarcinoma metastasis in an axillary lymph node without detectable primary tumor elsewhere. MRM of this case showed no definite mass or abnormal enhancement in both breasts and was diagnosed as occult breast cancer with axillary node metastasis. She was treated with axillary node dissection and systemic chemotherapy. One case had biopsy done and histopathology proved to be intraductal papillary carcinoma with foci of invasive tubular carcinoma. In the remaining eight cases, there was no lesion shown up after a period of follow - up time from 8 to 48 months (mean = 18.5).

The calculations of positive predictive value (PPV), negative predictive value (NPV), sensitivity, specificity and accuracy for the diagnosis of the breast disease were divided into three categories as shown in table 3, 4 and 5 since there were two different groups in MRI interpretation, one group (12 lesions) with MR signal time curve and the other (10 lesions) without signal time curve.

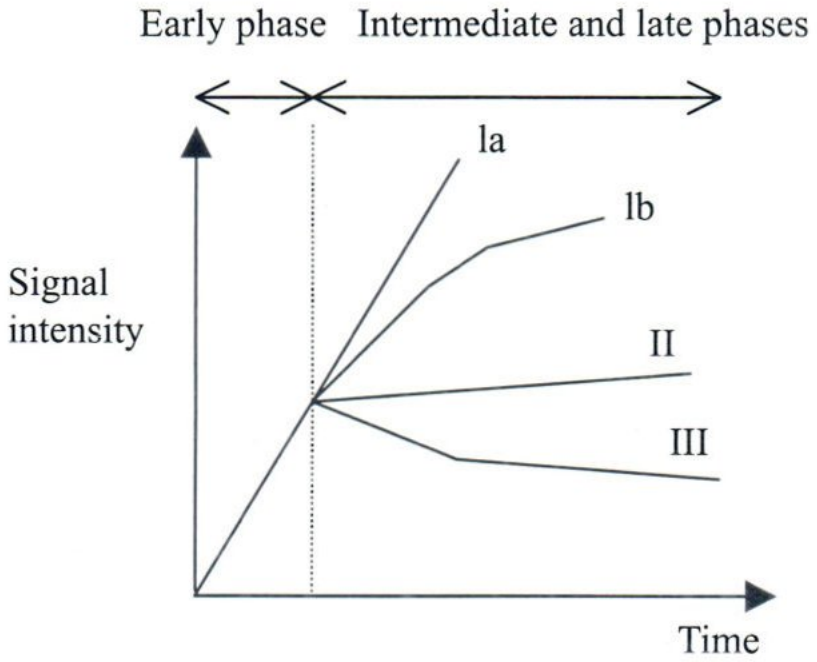

Fig. 1. Schematic drawing of the signal time curve types. Type I corresponds to a straight (Ia) or curved (Ib) line; enhancement continues over the entire dynamic study. Type II is a plateau curve with a sharp bend after the initial upstroke. Type III is a washout time course.[14]

Table 2. MRI score and breast lesion correlation.

No.	Age	coil	SI-T curve	MRI score	Conclusion	Remark
1.	34	shoulder	III	5	invasive ductal carcinoma	post conserving surgery
2.	62	"	I	1	benign (33 mo)	"
3.	50	breast	I	1	benign (16 mo)	"
4.	47	shoulder	-	2	benign (17 mo)	"
5.	52	"	-	5	invasive ductal carcinoma	"
6.	49	breast	I	1	benign (FNAC, 9 mo)	"
7.	43	"	III	5	invasive ductal carcinoma	"
8.	35	"	I	1	no malignant cell	post conserving surgery followed by mastectomy after 10 mo follow up.
9.	36	"	II	4	invasive ductal carcinoma	dense breasts
10.	55	shoulder	-	4	adenosis (needle-guide Bx, 59 mo)	asymmetrical breasts
11.	56	shoulder	-	5	invasive ductal carcinoma	male, mass in left breast
12.	54	body	-	1	adenocarcinoma of axillary node	left axillary mass
13.	26	breast	II	2	intraductal papilloma	right nipple discharge
14.	72	"	I	1	fibrofatty tissue (FNAC, 8 mo)	extensive fat necrosis
15.	45	body	-	2	intraductal papillary carcinoma with foci of invasive tubular carcinoma	left breast pain with bloody discharge
16.	45	shoulder	-	2	benign (48 mo)	palpable mass in Rt breast
17.	45	breast	II	1	benign (8 mo)	"
			II	2	benign (8 mo)	"
			II	2	benign (8 mo)	"
18.	54	shoulder	-	1	adenosis (FNAC, 57mo)	left breast pain, no palpable mass
19.	43	"	-	2	intraductal papilloma	right bloody discharge
20.	32	"	-	5	invasive ductal carcinoma	palpable mass

* The number behind the conclusion was the follow- up time interval.

Table 3. Data combined with and without signal time curve

	Malignant	Benign	Total
MRI +	6	1	7
MRI -	2	13	15
Total	8	14	22

Sensitivity = 75%, Specificity = 92.8%, PPV = 85.7%, NPV = 86.6%, Accuracy = 86.4%

Table 4. Data without signal time curve

	Malignant	Benign	Total
MRI +	3	1	4
MRI -	2	4	6
Total	5	5	10

Sensitivity = 60.0%, Specificity = 80.0%, PPV = 75.0%, NPV = 66.6%, Accuracy = 70.0%

Table 5. Data without signal time curve

	Malignant	Benign	Total
MRI +	3	0	3
MRI -	0	9	9
Total	3	9	12

Sensitivity = 100.0%, Specificity = 100.0%, PPV = 100.0%, NPV = 100.0%, Accuracy = 100.0%

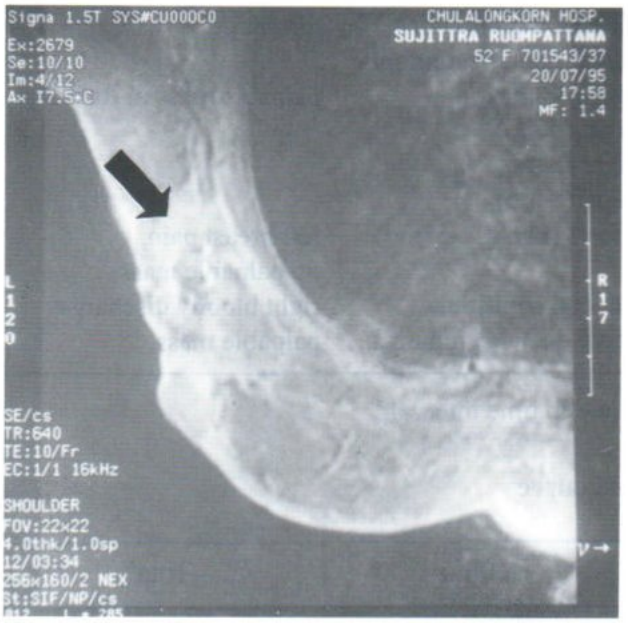

Fig. 1. Contrast MRM of right breast (T1WI with fat suppression) in axial view showed an irregular mass with rim enhancement (arrow), classified as malignant morphology

Fig. 2. Contrast MRM of right breast (T1WI with fat suppression) in sagittal view showed irregular lesion with heterogenous en hancement (arrow), classified as malignant morphology

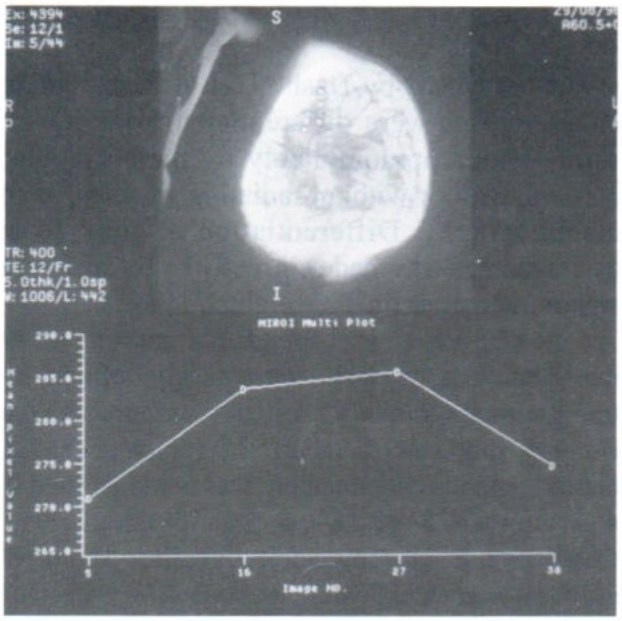

3A

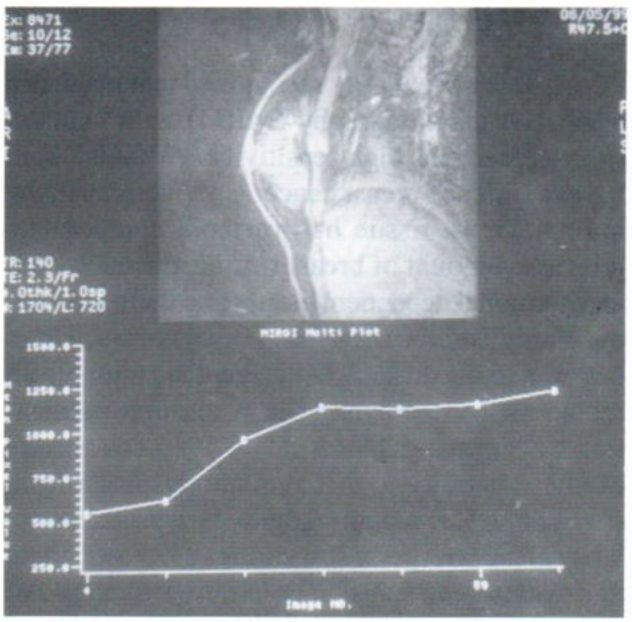

3B

Fig. 3 A,B. Contrast MRM with dynamic study showed washout signal time curve, type I (Fig.3 A), and plateau signal time curve type II (Fig. 3 B)

4A

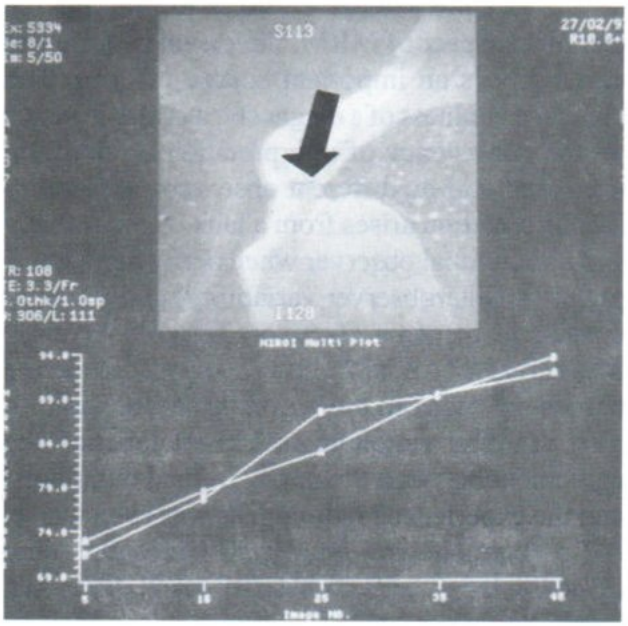

4B

Fig. 4A. Contrast MRM with subtraction in axial view showed a well defined homogenous hypersignal intensity mass in left breast (arrow), classified as benign morphology

Fig. 4 B. Contrast MRM with dynamic study showed a spiculated lesion (arrow) with type I signal time curve, classified as probably benign lesion (MRI score = 2)

DISCUSSION

It is now widely recognized that magnetic resonance mammography (MRM) with contrast enhancement has high sensitivity (93%-100%) in the detection of breast cancer.[2,10,11,12] Because the normal breast tissue has variable components related to amount of breast stroma, ductal system and hormonal dependent tissues and there are various fibroglandular patterns in each woman. These factors make it difficult to differentiate tumor from the breast parenchyma.[6] Since the first publication by Heywang SH. et al.[6] in 1986 concerning MRI's capability to differentiate dysplasia from carcinoma, MR mammography has gained popularity in the past years and various MRI sequences and techniques have been studied to improve diagnostic accuracy.[4,14-17] This capability is based on the fact that all carcinomas enhanced whereas dysplastic tissue enhanced slightly or not at all after Gd-DTPA injection.

Despite extensive efforts to improve the technical aspect of MRM, the extent of observer variability is an important source of error. The clinical usefulness of a diagnostic test also depends on the consistency of interpretation on different occasions and by different observers. Variability in interpretation arises from a lack of consistency by an individual observer when performing interpretation (interobserver variability) and a lack of consistent between observers (interobserver).[18] Mussurakis S. et al[18] showed only a moderate agreement between the two experienced radiologists in rating morphological characteristics, the agreement between the newly trained radiologist and the experienced radiologists was even worse. All readers showed good sensitivity in cancer detection but specificity was substantially lower.

MRM provides excellent anatomy and tissue morphology by using T1 and T2 weighted images. Including dynamic contrast study, MRM helps to clarify the tissue characteristics. Many reports have described the MRI features of benign and malignant lesions.[19-22] In the early reports of MRM by Dash N. et al.,[21] malignant breast masses were differentiated from benign solid lesions predominately by their irregular borders, with or without radiating spicules, as in mammography. Differentiation of solid from cystic masses was made correctly by the different signal intensities on T2 weighted images.[8]

LIU PF. et al.[17] found that margins of 44 malignant lesions (64%) were poorly defined, 25 malignancies showed well define borders. An irregular shape was found in 55 carcinomas (80%). Heterogeneous enhancement was demonstrated in 44 lesions (64%), and 8 lesions (12%) showed rim enhancement. Homogeneous or diffused contrast uptake was seen in 17 malignancies. They reported the sensitivity and specificity for the identification of breast cancer by MRM when based on qualitative morphological analysis alone were 83% and 54%. However the diagnostic accuracy of 71% was lower than that achieved when interpretation was based solely on quantitative data with a threshold of 90% (cut-off levels of % increase in SI at 1 minute post-contrast study). Combined quantitative and qualitative assessment yielded a considerably higher sensitivity, specificity and accuracy of 93 %, 74% and 85 % respectively.

Several years ago a dynamic MR imaging method was introduced.[12] Two concepts have evolved in attempt to improve diagnostic accuracy. First, high spatial resolution MRI is used to analyze the lesion's morphology including internal architecture. Second, fast imaging protocols with high temporal resolution have been suggested for analysis of the lesion's enhancement pattern.[14] Kuhl CK and colleagues[14] assessed the relevance of the signal intensity time course for the differential diagnosis of enhancing lesions in dynamic MR imaging of the breast. They studied 101 malignant and 165 benign lesions and found that the distribution of the curve types for breast cancers was type I, 8.9%; type II, 33.6%; and type III, 57.4%. The distribution of curve types for

benign lesions was type I, 83.0%; type II, 11.5%; and type III, 5.5%. The diagnostic indices for signal time curve were, sensitivity, 91%; specificity, 83%; and accuracy, 86%. They concluded that a type III time course is a strong indicator of malignancy and is independent of other criteria.

In our series, by using the MRI score as the parameter for establishing the diagnosis, the sensitivity, specificity and accuracy were 75.0%, 92.8% and 86.4% respectively. Furthermore, the lesions that we interpreted were analyzed into two groups; group I with signal time curve and group 2 without signal time curve. The sensitivity, specificity and accuracy were 60.0%, 80.0% and 75.0% in group I, 100%, 100% and 100% in group II, respectively. According to our one false positive case and two false negative cases in group I, there were only qualitative images. The dynamic study, subtraction images and SI-time curve were not performed at that time. We had found the difficulty in differentiation of malignant and benign lesions using only morphological qualitative images because the features between the benign and malignant lesions were overlapping and the diagnostic criteria for achieving optimal results were poorly defined. Consequencely, the signal time curve helped to distinguish the lesion precisely. Of the twelve lesions with signal time curves, five benign lesions were type I, two malignant lesions were type III. For the type II, there were three benign and one malignant lesions. Our study was concordant with Kuhl CK. and collegues[14] that type I indicated benignity and type III indicated malignancy. Since the type II could be presented in both benign and malignant lesions, combination of the MRI morphology and pattern of enhancement were necessary to judge the diagnosis.

In conclusion, contrast enhancement MRM with morphologic features and patterns of enhancement play important role in distinguishing the benign from malignant breast lesions that are indeterminated by mammography and ultrasonography. In our study, by adding the dynamic contrast study and signal time curve give not only confidence in diagnosis but also increase in sensitivity and specificity.

REFERENCES

1. Sardanelli F, Melani E, Ottonello C, Parodi RC, Imperiale A, Massa T, Parodi GC, Canavese G. Magnetic resonance imaging of the breast in characterizing positive or uncertain mammographic findings. Cancer detection and prevention 1998;22 (1):39-42.
2. Buchberger W, DeKoekkoek-Doll P, Obrist P, Dunser M. Value of MR tomography in inconclusive mammography findings. Radiologe 1997;37(9):702-9.
3. Heywang-Kobrunner SH, Viehweg P, Heinig A, Kuchler C. Contrast-enhanced MRI of the breast: accuracy, value, controversies, solutions. European Journal of Radiology 1997;24(2):94-108.
4. Murray AD, Redpath TW, Needham G, Gilbert FJ, Brookes JA, Eremin O. Dynamic magnetic resonance mammography of both breasts following local excision and radiotherapy for breast carcinoma. The British Journal of Radiology 1996;69:594-600.
5. Rieber A, Merkle E, Zeitler H, Gorich J, Kreienberg R, Brambs HJ, Tomczak R. Value of MR mammography in the detection and exclusion of recurrent breast carcinoma. J Comput Assist Tomogr 1997;21(5): 780-784.
6. Lewis-Jones HG, Whitehouse GH, Leinster SJ. The role of magnetic resonance imaging in the assessment of local recurrent breast carcinoma. Clinical Radiology 1991;43:197-204.
7. Dao TH, Rahmouni A, Campana F, Laurent M, Asselain B, Fourquet A. Tumor recurrence versus fibrosis in the irradiated breast: differentiation with dynamic gadolinium-enhanced MR imaging. Radiology 1993;187:751-755.

8. Humtaz H, Davidson T, Hall-craggs MA, payley M, Walmsley K, Cowley G, Taylor I. Comparison of magnetic resonance imaging and conventional tripple assessment in locally recurrent breast cancer. British Journal of Surgery 1997; 84:1147-1151.
9. Obdeijn IM, Kuijpers TJ, Van DP, Wiggers T, oudkerk M. MR lesion detection in a breast cancer population. Journal of Magnetic Resonance Imaging 1996;6(6): 849-54.
10. Drew PJ, Kerin MJ, Turnbull LW, Imrie M, Carletom PJ, Fox JN, Manson JR. Routine screening for local recurrence following breast-conserving therapy for cancer with dynamic contrast-enhanced magnetic resonance imaging of the breast. Annals of Surgical Oncology 1998;5(3): 265-70.
11. Davis PL, McCarty KS Jr. Sensitivity of enhanced MRI for the detection of breast cancer: new, multicentric, residual, and recurrent. European Radiology 1997;7 suppl 5:289-98.
12. Fisher U, Kopka L, Grabbe E. Breast carcinoma: effect of preoperative contrast-enhanced MR imaging on the therapeutic approach. Radiology 1999;213(3):881-888.
13. Heywang SH, Hahn D, Schmidt H, Krischke I, Eiermann W, Bassermann R, Lissner J. MR imaging of the breast using Gadolinium-DTPA. J Computer Assist Tomogr 1986;10(2):199-204.
14. Kuhl CK, Mielcareck P, Klaschik S, Leutner C, Wardelmann E, Gieseke J, Schild HH. Dynamic breast MR imaging: Are signal intensity time course data useful for differential diagnosis of enhancing lesion? Radiology 1999;211(1): 101-110.
15. Holden A, anderson JE, Ives FJ, Taylor D, Wylie EJ, Adamson R. Breast MRI: early experience with a 3-D fat-suppressed gradient echo sequence in the evaluation of breast lesions. Australian Radiology 1996;40(4):391-7.
16. Hulka CA, Smith BL, Sgroi DC, Tan L, Edmister WB, Semple JP, Campbell T, Kopans DB, Brady TJ, Weisskoff RM. Benign and malignant breast lesions: differentiation with echo-planar MR imaging. Radiology 1995;197:33-38.
17. Kerslake RW, Fox JN, Carleton PJ, Imrie MJ, Cook AM, Bowsley SJ, Horsman A. Dynamic contrast-enhanced and fat suppressed MR imaging in suspected recurrent carcinoma of the breast: preliminary experience. The British Journal of Radiology 1994;67(804):1158-1168.
18. Mussurkis S, Ruckley DL, Coady AM, Turnbull LW, Horsman A. Observer variability in the interpretation of contrast enhanced RMI of the breast. The British Journal of Radiology 1996;69(827):1009-1016.
19. Nunes LW, Schnall MD, Orel SG, Hochman MG, Langlotz CP, Reynolds CA, Torosian MH. Breast MR imaging: Interpretation model1. Radiology 1997; 202:833-841.
20. Orel SG, Schnall MD, LiVolsi VA, Troupin RH. Suspicious breast lesions; MR imaging with radiologic-pathologic correlation. Radiology 1994;190:485-493.
21. Dash N, Lupetin AR, Daffner RH, Deeb ZL, Sefczek RJ, Schapiro RL. Magnetic resonance imaging in the diagnosis of breast disese. AJR 1986;146:119-125.
22. El Yousef SJ, O'Connell DM, Duchesneau RH, Smith MJ, Hubay CA, Guyton SP. Benign and malignant breast disease: magnetic resonance and radiofrequency pulse sequences. AJR 1985;145:1-8.

SPIGELIAN HERNIA: REAL-TIME SONOGRAPHIC DIAGNOSIS

Koakait VIVITMONGKONCHAI

ABSTRACT

The diagnostic potential of real-time sonography in detecting a clinically unrecognized case of spigelian hernia is illustrated and discussed. Due to its rarity and nonspecific presentation, spigelian hernia is often misdiagnosed clinically. Real-time sonography can provide the correct diagnosis by demonstrating dynamic sliding of hernial content through the peritoneal and muscular defect along the spigelian line in lower anterior abdominal wall.

INTRODUCTION

Spigelian hernia is an uncommon anterior abdominal wall hernia that developed at either side, along the linea semilunaris, usually inferior to umbilicus. Clinical diagnosis of spigelian hernia poses greater difficulties than treatment. The clinical presentation varies, depending on the side, contents, degree and type of herniation. The compliants range from vague intermittent abdominal pain with or without palpable mass to acute symptoms related to intestinal obstruction and strangulation or incarceration of hernial contents. Most hernias, if not large enough, are overlooked because they are masked by the intact external aponeurosis and subcutaneous fat especially in obese patients. Because of its nonspecific presentation and difficulty in clinical diagnosis, ultrasound study can be significantly helpful in preoperative diagnosis.

CASE REPORT

A 44-year-old man complained of left lower quadrant pain for one day without associated nausea, vomiting, constipation or diarrhea. Physical examination showed mild focal tenderness with ill-defined, mass-liked sensation over left lower abdomen.

The provisional diagnosis was acute diverticulitis with possible abscess and ultrasound study was ordered as a screening examination. The sonoscan revealed a hyperechoic mass, 3.17x2.12x2.84 cm. in size, locating in anterior peritoneal cavity with partly herniated through a defect of aponeurosis to lie immediately beneath anterior abdominal wall muscle. [fig. 1] The mass appeared to be increased in size and herniated more anteriorly when the patient was told to strain. [fig. 2] This dynamic procedure was reproducible and clearly demonstrated by real-time sonography. Due to its typical location and dynamic nature, the mass was diagnosed as spigelian hernia. The patient underwent laparotomy and a hernia sac was discovered through the spigelian defect. The sac contained gangrenous appendices epiploicae, which was resected. Then the defect was repaired. Postoperatively, the patient did well with complete recovery from the presented symptoms.

Department of Radiology, Faculty of Medicine, Thammasat University, Rangsit Campus, Thailand

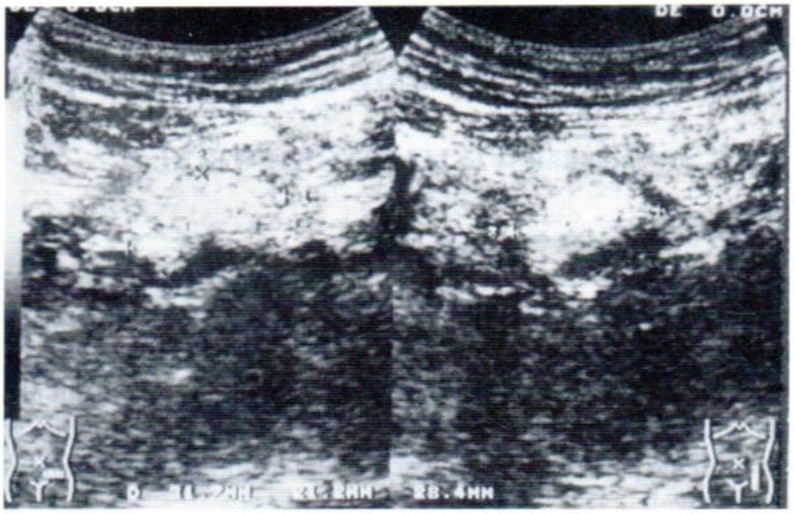

Fig. 1 A hyperechoic mass in anterior peritoneal cavity partially herniated through spigelian defect on left side of anterior abdominal wall.

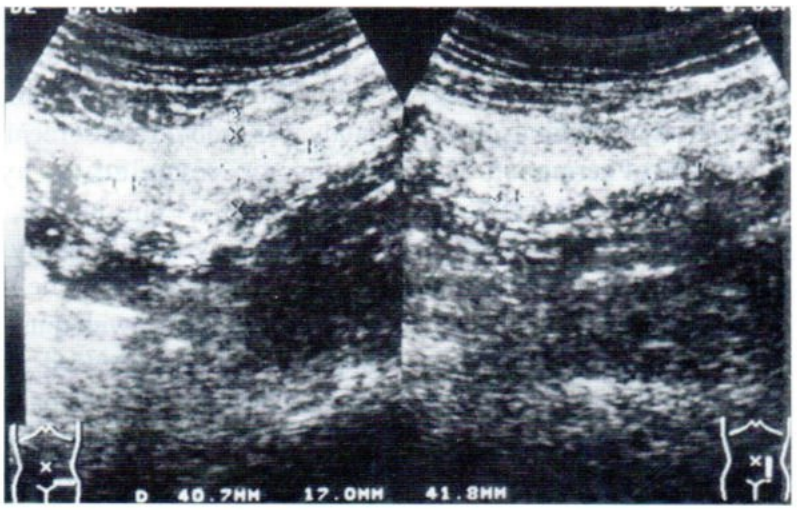

Fig. 2 With abdominal strain, the mass herniated more anteriorly through the abdominal wall defect.

DISCUSSION

Spigelian hernia is an uncommon, acquired anterior abdominal wall hernia that occurs through a defect in the spigelian aponeurosis. The spigelian aponeurosis is the part of aponeurosis that lies lateral to the rectus abdominis muscle and medial to linea semilunaris, which is the line forming and marking the transition from muscle to aponeurosis of the three abdominal muscles of anterior abdominal wall-namely external oblique, internal oblique and transversus abdominis.[1] In its upper three fourths, the fused aponeurosis of these three muscles splits medially to form the anterior and posterior rectus sheath. At the lower fourth, the aponeurosis passes medially to cover only the anterior surface of the rectus muscle. This anatomic transition is marked by linea semicircularis.[2] Most hernias occur at the widest part of the aponeurosis just below the level of umbilicus in the region of linea semicircularis.[3,4] On rare occasions, such hernias have been occurred caudal and medial to the inferior epigastric artery which are called low spigelian hernias.[1]

Spigelian hernias occur at any age but more commonly in the eldery.[1,3,5] The ratio of incidence is equal in both men and women.[1,2,3,5] They developed with almost equal frequency on either side and occasionally be bilateral[1,3,5] The clinical presentation varies, depending on the sides, contents, degree and type of herniation. The hernial sac contents are usually omentum and/or segment of small bowel or colon but other structures such as stomach, ovary, Meckel's diverticulum and even endometrial tissue have been reported.[1,3,5] Spigelian hernias represent less than 2% of anterior abdominal hernias[3,5] and because of common delays in the diagnosis, they are associated with a higher risk of bowel strangulation than other abdominal wall hernias.[2,3,5] Due to their rarity, nonspecific presentations and difficulty in clinical diagnosis, many physicians are unaware of these hernias. As a result, radiologic studies play an important role in giving the correct diagnosis. Spigelian hernias rarely show any abnormalities on scout abdominal films except that they cause small or large bowel obstruction. Since most of the spigelian hernias donot contain intestinal loops, the plain abdominal film findings are usually absent or nonspecific. They can be more specifically diagnosed with small bowel contrast study or barium enema if they do contain the intestinal segment in the hernial sacs.[3,5] With newer imaging modalities as real-time ultrasound, computerized tomography and magnetic resonance imaging, spigelian hernias are easier to be diagnosed. The added advantage of these high resolution studies is evident in as much as omental fat herniation can be diagnosed even when there is no intestinal herniation. Ultrasound is a good screening examination because of its availability, cheaper cost and lack of radiation hazard. Moreover; it provides good imaging resolution, multiplanar views and real-time display on specific maneuvers. Spigelian hernia can be diagnosed by demonstration of a hernial orifice in the spigelian aponeurosis, on an intramurally located hernial sac and on sac content in the form of intestine or omentum. The hernial orifice is visualized as a defect in the echo line from the aponeurosis. Since the hernia is sliding in nature, it can be diagnosed more confidently by using several provocative maneuvers that increase intraabdominal pressure such as the Valsalva maneuver, abdominal strain, upright position, coughing, etc.[2] The great benefit of ultrasound study is its ability to demonstrate this motion graphically in real time. This capability is not possible with the static scans of other imaging modalities. As shown in this reported case, the hernia was augmented by abdominal strain which help in making the diagnosis more specifically. Some anterior abdominal wall pathologies and intraabdominal processes that are superficial in peritoneal cavity

may produce similar sonographic appearance. Among them are abdominal wall lipoma, abscess, rectus sheath hematoma or seroma, and peritoneal or omental tumor implants.[4,5,6] The hernial sac can be confused with lipoma of the abdominal wall when the external oblique aponeurosis is also defective.[7] When the hernia is incarcerated, the provocative maneuvers may fail to demonstrate sliding of hernial contents. Nevertheless; with careful attention to the abdominal wall defect at specific location, the diagnosis of spigelian hernia can be made in most cases. Further studies can be done in problematic cases which should be judged on case-by-case basis.

In conclusion, real-time sonography has shown to be very helpful and effective in the diagnosis of spigelian hernia which is difficult to diagnose clinically.

REFERENCES

1. Spagen L: Spigelian Hernia. World J Surg 1989;13:573-580
2. Mufid MM, Abu-Yousef MM, Kakish ME, Urdaneta LF, Al-Jurf AS: Spigelian Hernia: Diagnosis by High-Resolution Real-time Sonography. J Ultrasound Med 1997;16:183-187.
3. Balthazar EJ, Subramanyam BR: Radiographic Diagnosis of Spigelian Hernia. Am J Gastroenterol 1983;78:525-528.
4. Fried AM, Meeker WR: Incarcerated Spigelian Hernia. Ultrasonic Differential Diagnosis. AJR 1979;133:107-110.
5. Balthazar EJ, Subramanyam BR, Megibow A: Spigelian Hernia: CT and Ultrasonography Diagnosis. Gastrointest Radiol 1984;9:81-84.
6. Sutphen JH, Hitchcock DA, King DC: Ultrasonic Demonstration of Spigelian Hernia. AJR 1980;134:174-175.
7. Lee HM, Cohen AJ:CT Imaging of Abdominal Hernias. AJR 1993;161:1209-1213.

SEVERE HYDROURETER MIMICKING VESICAL CATHETER BALLOON AT SONOGRAPHY

Dr. M. A. Taher, Director

Indexing words : Hydroureter, Ultrasonography, Renography.

INTRODUCTION

Most of the patients of painful hematuria are benefitted from radionuclide renogram and ultrasonography.[1-4] Radiation dose from the isotope used in renography is very small : one-hundredth of that from intravenous urography (IVU).

Sonography is a non-invasive and non-ionizing procedure which has become very much popular in the investigation of various diseases. However, one must be careful and cautious to interpret the images, for example, cystitis may sometimes mimic bladder cancer on sonography.[5]

CASE REPORT

A boy of 8 years came with complains of pain in left loin and hematuria. Radionuclide renogram with Tc-99m DTPA showed left-sided obstructive uropathy. Ultrasonography showed severe hydronephrosis and hydroureter on left side, a balloon-like structure was seen in the lumen of urinary bladder, but the patient was never catheterized: On careful scanning it was seen to be continuous with the left hydrourerter. We report this case considering its rarity. (Fig.1)

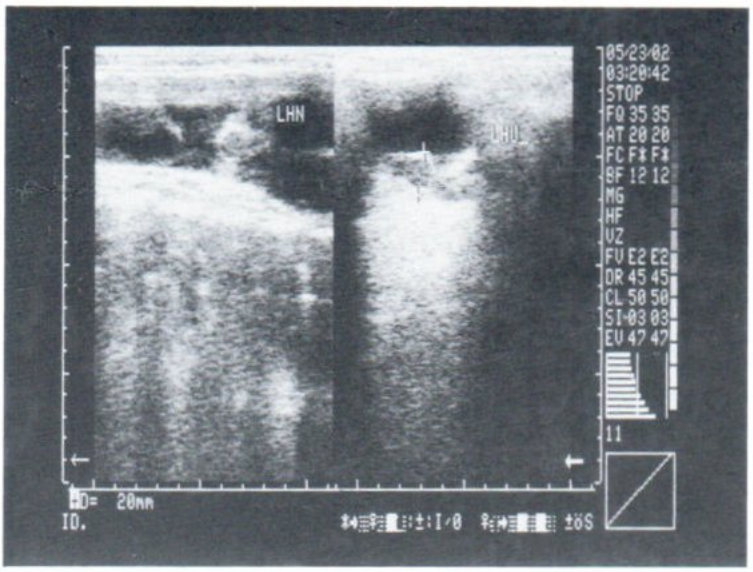

Fig. 1 LHU = Left hydroureter,
LHN = Left hydronephrosis

Nuclear Medicine Centre, Rangpur, Bangladesh.

REFERENCES

1. Taher MA. Complementary role of radionuclide renogram and nephrosonogram. Bangladesh J Nucl. Med. 2:13-14, 1999.
2. Spencer J, Lindsell D, Mastorakou I. Ultrasonography compared with intravenous urography in the investigation of adults with hematuria. Br. Med. J 301: 1074-1076, 1990.
3. Taher MA. Urogenital anomalies : case reports. Bangladesh J Nucl Med 2:38-41, 1999.
4. McGahan JP, Richards JR, Jones CD, Gerscovich EO. Use of ultrasonography in the patient with acute renal trauma. J Ultrasound Med. 18:207-213, 1999.
5. Taher MA, Afroz S. Cystitis mimicking bladder cancer on sonography. Amer J Roentgenol (AJR) 151:1252-1253, 1998.

SOLITARY OSTEOCHONDROMA OF THE THORACIC SPINE WITH SPINAL CORD COMPRESSION; A CASE REPORT

Waneerat GALASSI, M.D.

ABSTRACT

Osteochondromas are common benign bone tumors that rarely occur in the axial skeleton. In the solitary type or multiple osteochondromas, neurological complications such as spinal cord compression has rarely been reported. A case of 53-year-old man with an osteochondroma of T10 lamina and spinal cord compression is reported. Plain radiographs, myelography, and computed tomography were used in the preoperative assessment of the lesion. Laminectomy with decompression of neural elements is the treatment of choice for intracanicular osteochondromas.

INTRODUCTION

Osteochondromas are common benign bone tumors, although they are actually hyperplastic or dysplastic bone disturbance originating from displaced or aberrant cartilage of the growth plate. Solitary and multiple osteochondromas affect male patients more frequently than female patients and most patients are 20 years old of age or younger.[1,2] This is a report of an unusual case of solitary osteochondroma of the lamina of T10 signaled by spinal cord compression in the sixth decade.

CASE REPORT

A 53-year-old man had experienced a slowly progressive onset of weakness in the left lower extremity for 2 months. Physical examination showed generalized weakness of the extremities, greater on the left, with decreased sensation of both legs. Retrospective review of plain radiographs (Figure 1A) showed an abnormal bony density projecting centrally from the left side of the posterior element of T10. The patient underwent myelographic examination (Figure 1B), which showed this extradural lesion causing spinal block at T10. Computed tomography after myelography (Figure 2A,B) confirmed a left posterior extradural bony mass from the left lamina of T10 extending caudally and displacing the spinal cord and thecal sac to the right anterolateral aspect. No soft tissue mass was present. The patient underwent T10-T11 laminectomy with decompression of neural elements.

Histopathologic examination (Figure 3) was consistent with an osteochondroma.

Faculty of Medicine, Naresuan University, Phitsanulok, 65000 Thailand.

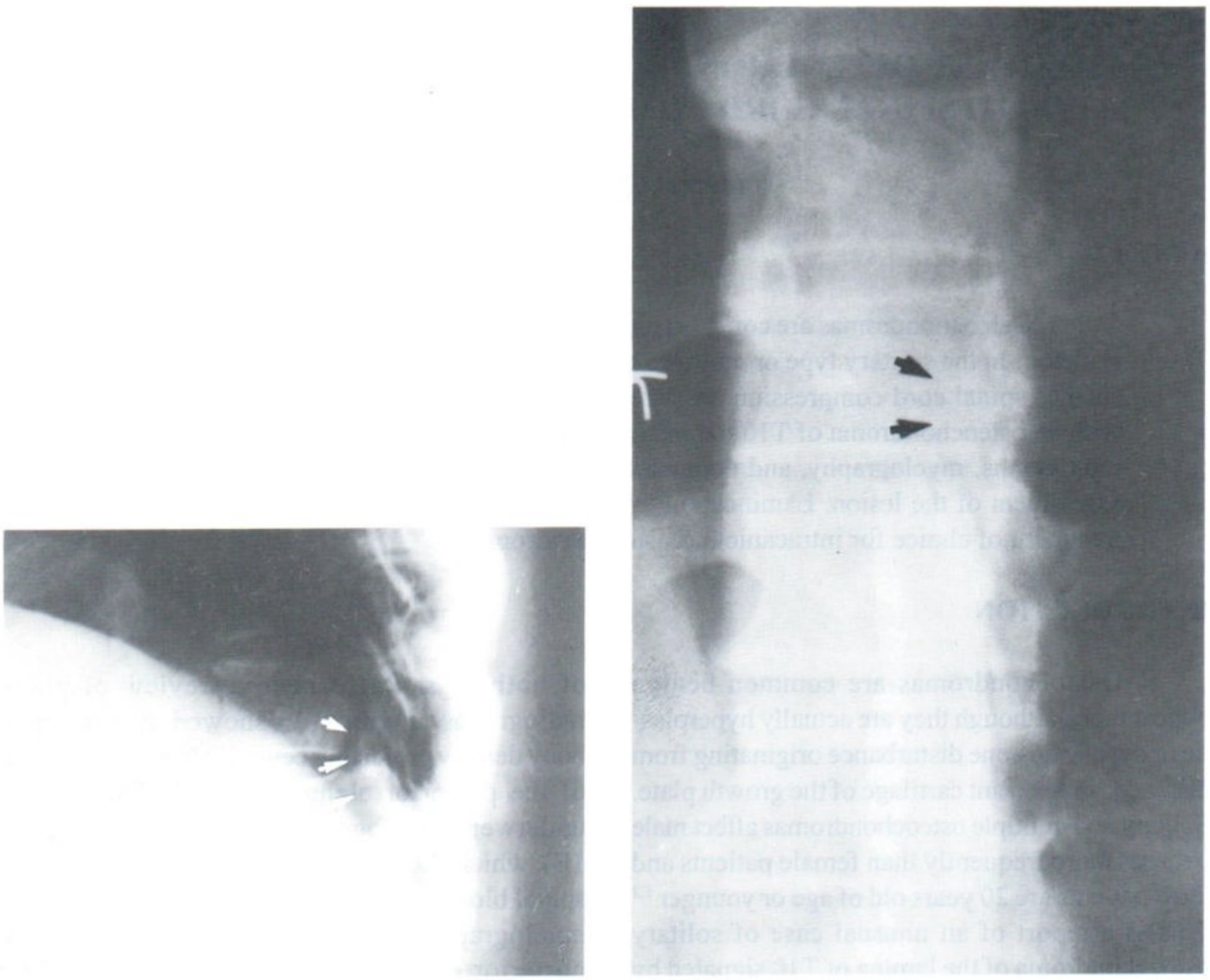

1A 1B

Fig. 1 Lateral thoracic radiograph (A) shows an ossified region(arrowheads) at the left side of the posterior element of T10 without optimal delineation of marrow and cortical continuity with the underlying bone. Thoracic myelogram (B) shows this extradural lesion causing spinal cord compression.

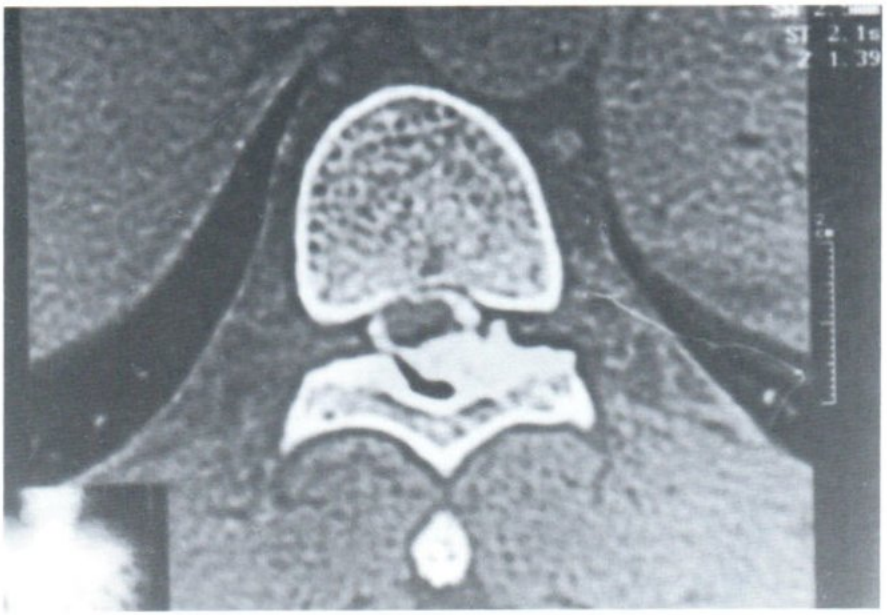

2A

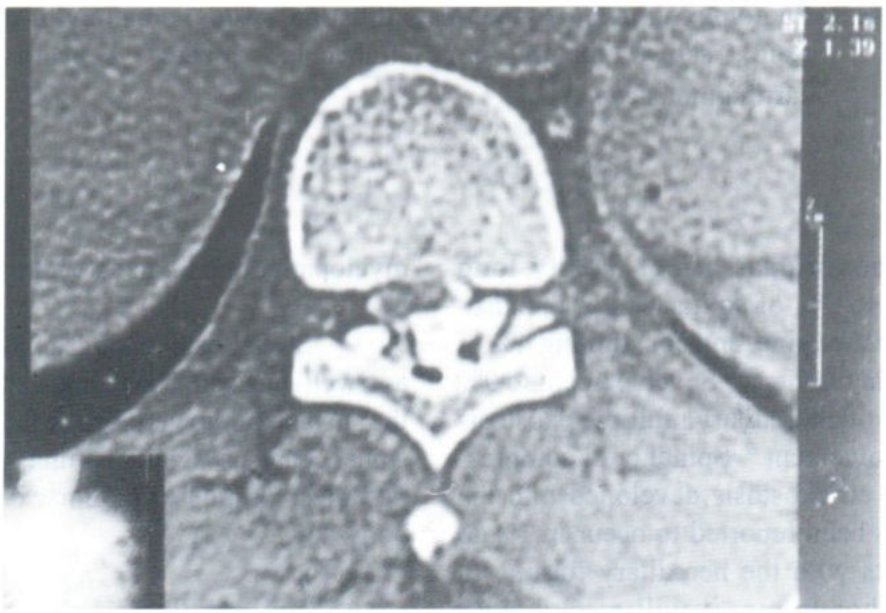

2B

Fig. 2A, B Axial computed tomographic images show an exophytic calcified lesion arising from the left T10 lamina.

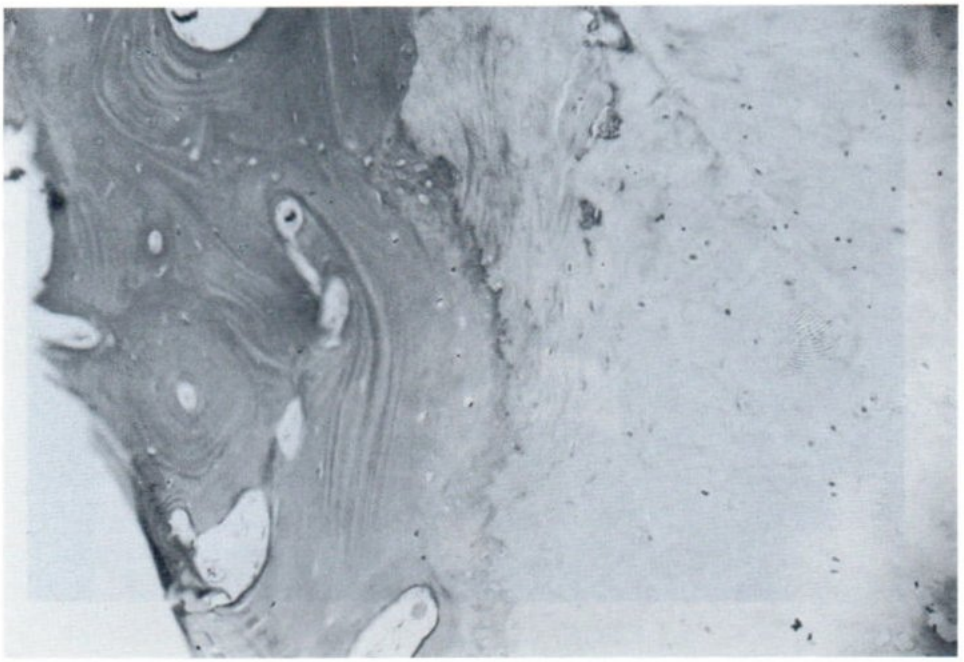

Fig. 3 Photomicrograph (original magnification, x100; hematoxylin-eosin stain) shows mature bone trabeculae located beneath the cartilaginous cap.

DISCUSSION

Osteochondromas affect mostly long bones,only 2% to 3% of solitary osteochondromas originate in the spine, and constituting 4% of all solitary spinal tumors.[2-5] Seven percent to 9% of the patients with hereditary multiple exostosis have spinal involvement.[6] Spinal cord compression caused by an exostosis developed into the spinal canal has been reported to occur in 1% to 2.5% of patients with the hereditary form.[7] In solitary osteochondroma, it will rarely cause neurological deficits. In the recent literature, osteochondroma of the thoracic spine with scoliotic deformity has also been reported.[8]

A 53-year-old man presented with a solitary osteochondroma of the thoracic spine. Surprisingly is the development of this neoplasm in this age group. The oldest case in the literature is a 73-year-old woman coming with cervical myelopathy due to an osteochondroma.[9]

Spinal osteochondromas typically appear as a well-corticated bone mass usually arising from the surface of the vertebra or from any wall of the spinal canal, especially lamina, spinous processes, pedicles, or posterior cortex of the vertebral body.[5,10]

The radiologic hallmark of osteochondroma is the continuity of the lesion with the marrow and cortex of the underlying bone and it's type may be pedunculated or sessile form. Small osteochondromas related to the lamina or pedicle particularly those extending into the spinal canal are difficult to detect on plain radiographs, so a further imaging workup is required.[2,7,11] In 15% of cases of spinal osteochondroma, the radiographs are considered normal.[3,12,13] Myelography will

show evidence of extradural compression in almost all patients with neurologic signs or symptoms.[14]

Thin-section computed tomography is the imaging modality of choice in defining the bony nature of the lesion, tumor's extent and its relationship to the vertebral and neural elements of the spine.[14-16]

Magnetic resonance imaging is more useful than computed tomography in defining an extradural component of the tumor and dural compression.[17] When the cartilaginous cap completely calcified, osteochondromas tend to stop growing, but growth may persist after the closest epiphyseal plate has closed.

Sarcomatous transformation of solitary osteochondromas occurs in less than 1% of cases. However, a thick cartilaginous cap (> 1 cm) in an adult should raise the suspicion of an exostotic chondrosarcoma. In conclusion, osteochondromas of the thoracic spine may cause spinal cord compression. Thin-section computed tomography is necessary for evaluating the origin,size, and characteristics of the tumor. In this case, the treatment of choice involved laminectomy with decompression of neural elements.

ACKNOWLEDGEMENT

I would like to thank all the staff of the Department of Radiology and Pathology, Bhuddhachinarach Hospital, Dr Julintorn Somran, and Dr Monton Galassi for the source of all informations required for the study.

REFERENCES

1. Labram EK, Mohan J. Diaphyseal aclasis with spinal cord compression: Report of two cases and review of the literature. J Neurosurg 1996; 84: 518-521
2. Roblot P, Alcalay M, Cazenave-Roblot F, Levy P, Bontoux D. Osteochondroma of the thoracic spine: Report of a case and review of the literature. Spine 1990;15: 240-243.
3. Albrecht S, Crutchfield JS, Segall GK. On spinal osteochondromas. J Neurosurg 1992;77: 247-252
4. Calhoun JM, Chadduck WM, Smith JL. Single cervical exostosis: Report of a case and review of the literature. Surg Neurol 1992;37:26.
5. Khosla A, Martin DS, Awwad EE. The solitary intraspinal vertebral osteochondroma. An unusual cause of compressive myelopathy: Features and literature review. Spine 1999;24:77.
6. Murphey MD, Andrews CL, Flemming DJ, et al. Primary tumors of the spine: radiologic-pathologic correlation. Radiographics 1996;16:1131.
7. Kulali A, Vural A, Fiskeci C. Solitary vertebral osteochondromas causing spinal cord compression. Neuro Orthopedics 1991;11:109-116.
8. Jose Alcaraz Mexia M, Izquierdo Nunez E, Santonja Garriga C, et al. Osteochondroma of the thoracic spine and scoliosis. Spine 2001;26:1082-1085.
9. Kaneko K, Yasuma M, Yanase H. Cervical myelopathy due to an osteochondroma in a 73-year-old female. The oldest case in the literature. Bull Hosp Jt Dis 2000; 59:106-110.
10. El Quessar A, Chakir N, El Hassani MR, et al. Exostose vert?brale et compression médullaire. J Neuroradiol 1998;25:253.
11. Loftus CM, Rozario RA, Prager R, Scott M. Solitary osteochondroma of T4 with thoracic spinal cord compression. Surg Neurol 1980;13:355-357.
12. Jackson A, Hughes D, Forbes W, et al. A case of osteochondroma of the spine. Skeletal Radiol 1995;24:235-237.

13. Palmer FJ, Blum PW. Osteochondroma with spinal cord compression. J Neurosurg 1980;52:842-845.
14. Cooke RS, Cumming JK, Cowie RA. Osteochondroma of the cervical spine: Case report and review of the literature. Br J Neurosurg 1994; 8: 359-363.
15. Fanney D, Tehranzadeh J, Quencer RM, et al. Osteochondroma of the cervical spine: Case report. Skeletal Radiol 1987; 16:170-174.
16. Marchad EP, Viliemure JG, Rubin J, et al. Solitary osteochondroma of the thoracic spine presenting as spinal cord compression: A case report. Spine 1986;11:1033-1035.
17. Cherubino P, Benazzo F, Castelli C. Osteochondroma of the cervical spine. Ital J Orthop Traumatol 1991;17:131-134.

TWIN NON-IMMUNE HYDROPS FETALIS (NIHF).

Dr. M.A. Taher

ABSTRACT

Non-Immune hydrops fetalis (NIHF) is a clinical entity that affects non-Rh-sensitized pregnancies and is characterized by fetal anasarca, placental edema, and often fetal serious effusions. It was first described in 1943 by E.L. Potter.[1] Recently we diagnosed NIHF in a twin and reporting it as a rare case.

Indexing Words: Twin pregnancy, Hydrops fetalis.

CASE REPORT

A muslim multiparous female of 31 yrs. gravida 3rd, came with a history of 7 months' amenorrhea complaining of ankle edema and unusual fundal height. Ultrasonographic examination (Concept 2000 U.K.) was performed and showed a twin pregnancy of about 28 wks. One fetal head was high up on right side, the other was lying low on left side. Biparietal diameter (BPD) was 67.1mm., femur length (FL) was 46 mm., both corresponding to a about 28 wks. of gestation. Both fetal hearts were beating regularly at 147 per minute, Abnormal fluid collections were noted in fetal scalp, pericardial and peritoneal spaces (Fig. 1). She had two sons of ages 8 and 6 years, both were delivered normally at home and both are having normal health. Therefore we label the case non-immune hydrops fetalis (NIHF). Unfortunately the patient was lost to followup.

Fig. 1 Ultrasonography of the case of non-immune hydrops fetalis.

DISCUSSION

In 1943, non-immune hydrops fetalis represented less than 20% of all cases of hydrops fetalis, however, since the advent of effective prophylaxis against Rh(D) sensitization, the relative frequency of non-immune hydrops fetalis has risen to 90%.[2] The incidence of non-immune hydrops fetalis ranges from one in 14,000 to one in 7000.[3-5] The mortality rate for non-immune hydrops fetalis ranges from 50-98%.[3-6] The complications of NIHF are tabulated below (Table 1).

Nuclear Medicine Centre, Rangpur, Bangladesh.

Table 1. Complications of NIHF

Complications	Frequency
Polyhydramnios	50-75 %
Pregnancy-induced hypertension	15-46 %
Maternal anemia	7-45 %
Maternal hypoalbuminemia	6-67 %
Fetal arrhythmia	15 %

In 1963, Liley pioneered the intrauterine transfusion for the treatment of severe red cell alloimmunization. In 1985, Daffos described the presently used method of ultrasound-guided percutaneous umbilical cord blood sampling and intravascular transfusion. In 1991, Anandkumar et al claimed 85% success rate in cases of non-immune hydrops fetalis by administering digoxin 25 picomicrogram and furosemide 0.5 mg per kg daily for 10 days.[7]

A case of NIHF caused by severe fetal aortic stenosis and endocardial fibroelastosis was treated successfully by transplacental digitalization (oral loading dose of 0.8 mg digoxin to the mother three times at 8-h intervals for 2 weeks and therapeutic levels 2 mg/ml were maintained by oral digoxin therapy).[8-10] As our case was lost to follow-up we could not try any therapy.

REFERENCES

1. Potter EL. Universal edema of the fetus unassociated with erythroblastosis. Am J Obstet Gynecol 46:130,1943.
2. Warsof SL, Nicolaides KH, Rodeck C. Immune and non-immune hydrops. Clin Obstet Gynecol 29:533,1986.
3. Etches PC, Lemons JA. Nonimmune hydrops fetalis : Report of 22 cases including three siblings. Pediatrics 64:326,1979.
4. Graves GR, Baskett TF. Nonimmune hydrops fetalis. Antenantal diagnosis and management. Am J Obstet Gynecol 148: 563,1984.
5. Im SS, Rizos N, Joutsi P et al. Nonimmunologic hydrops fetalis. Am J Obstet Gynecol 148 : 566, 1984.
6. Hutchinson A, Drew JA, Yu V et al. Nonimmunologic hydrops fetalis : A review of 61 cases, Obstet Gynecol 59: 247,1982.
7. Anandkumar C, Wong YC. Invesive procedures in fetal medicine. In Malhotra N (ed.) Ultrasound in Obstetrics & Gynecology, 3rd ed. PP 184-189, Jaypee Bros. New Delhi, 2001.
8. Maeda H. Shimokawa H, Nakano H. Effects of intrauterine treatment on non-immunologic hydrops fetalis. Fetal ther 3: 198-209,1988.
9. Schmider A, Henrich W, Dahnert I, Dudenhausen JW. Prenatal therapy of non-immunologic hydrops fetalis caused by severe aortic stenosis. Ultrasound Obstet Gynecol 16:275-278,2000.
10. Chavkin J, Kupfersztain C, Ergaz Z, Guedj P, Finkel AR, Stark M. Successful outcome of idiopathic nonimmune hydrops fetalis treated by maternal digoxim. Gynecol Obstet Invest 42:137-139,1996.

FOLLOW-UPS OF CONGENITAL HYPOTHYROIDISM

Dr. M. A. Taher

ABSTRACT

Brain development depends on thyroid hormones, the delay in starting treatment of hypothyroidism leads to a permanent mental impairment which will be more severe, the longer the delay of the treatment. So neonatal screening for congenital hypothyroidism is very important, as is being done in other countries. Congenital hypothyroidism is common in northern Bangladesh, but can be cured, if treated early as documented by the six cases presented hear.

Key words : Congenital hypothyroidism

MATERIALS AND METHODS

Among about 6000 patients at the Institute of Nuclear Medicine Dhaka, Nuclear Medicine centres at Dinajpur & Rangpur, examined by various radioisotope techniques e.g. Radioiodine Uptake (RAIU), Thyroid scan, RIA of T3, T4, & TSH. We looked for congenital hypothyroidism.

RESULTS : Results are presented case-wise.

CASE 1

A girl, 4 years in chronological age, but 2 years in bone age (2 carpal bones present), with dull look came at N.M.C, Dinajpur in 1991. Her mother complained that the baby was constipated, her appetite was poor and her growth was retarded both physically and mentally---she could not walk and talk. Her radioiodine uptake and serum levels of thyroid hormones were low (RAIU 2 h. 1.88%, 24 h. 0.34%), (Table-1). She was given thyroxine tablets at first 12.5 micrograms/day and gradually the dose was increased to 25 mcg/d, then 50 mcg/d in 1995. Since then she was being followed up at N.M.C, Rangpur --- she was of quite normal look, her memory became good, bone age was 7 years in 1995, her school performance was also quite satisfactory (stood 9th among 45 students).

She was taking 75 mcg/day thyroxine (occasionally irregular) since 1998 and experienced menarche at 12 years of age in Apr. 1999. Her secondary sex characters were also normal. She was advised to increase thyroxine to 100 mcg daily on 25.10.99, due to high TSH level.

CASE 2

Daughter of a physician started thyroxine therapy at 5 mo. of age, had irregular medication due to nonavailability, however, physically & mentally well, started menarche at 13y. 6m. (Sep. 1999). In Sep. 1998 her T_3 was 1.7 nmol/L, T_4 was 188 nmol/L, TSH was 56.5 mIU/L and increased the dose of thyroxine to 125 mcg/day.

CASE 3

Another girl of 18 yrs. age came here for

Nuclear Medicine Centre, Rangpur, Bangladesh.

thyroid investigations with a history of thyroxine therapy for last 14 yrs. for congenital hypothyroidism she was taking 250 micrograms of thyroxine daily, married on 5.12.99, but having occasional polymenorrhea and constipation probably due to irregular medication. On 19.12.99 her T_3 was 1.8 nmol/L, T4 was 375 nmol/L, TSH was 0.5 mlU/L and she was advised to reduce the dose of thyroxine to 150 mcg/day.

CASE 4

A girl of age 12 yrs. treated by Carbamazepine and clobazam for epilepsy and dull memory, had T_3 = 1.01 nmol/L, T_4 = 18 nmol/L and TSH = 115 mlU/L on 27.11.96 and started thyroxine therapy (100 mcg/day), she improved her intelligence and had menarche in 1997 and increased the dose of thyroxine to 150 mcg/day. On 23.12.98 her T_3 was 1.9 nmol/L, T_4 was 42 nmol/L and TSH was 2.5 mlU/L.

CASE 5

A girl of age 6 months presented with constipation of one week in June 1999. Her T_3 was 0.35 nmol/L, T_4 was 9 nmol/L, and TSH was 87.5 mlU/L. She was improved by thyroxine (12.5 mcg/day), as confirmed by follow-ups done at 3 and 6 months of intervals.

CASE 6

A female baby of age 4 months presented with oliguria and constipation on 4.1.2000. Her T_3 was 0.15 nmol/L, T_4 was 7 nmol/L, and TSH was 100 mlU/L. She was improved by thyroxine tablets 12.5 mcg/day.

Table 1. Hormone levels of case 1

Date	T_3 NR 0.8-3.16 nmol/L	T_4 NR 64.5-152 nmol/L	TSH NR 0.3-6 mlu/L
17. 2 .91	0.94	<20	---
13. 8 .98	2	115	95
25.10 .99	1.7	114	100

NR = Normal range.

DISCUSSION

In 1908, McCarrison first described the two forms of cretinism- hypothyroid and neurologic.[1] Incidence of congenital hypothyroid was 1 in every 3000 to 6000 live births in Europe (1979)[2] and America (1976)[3] In iodine-sufficient populations about 1 in 4000 neonates has congenital hypothyroidism usually from inadequate thyroid development,[4] screening program was advised[5] but not yet implemented fully.[6] Dose of thyroxine is to be monitored regularly-it should always be taken as a single daily dose as it has a plasma half-life of about seven days. The correct dose of thyroxine is that which restores serum TSH to normal. Hormonal assays should be done at least as often as 4 weeks after each change in thyroxine dosage as well as 2 and 6 wks. after initiation of therapy and at 3, 6, 9, 12 and 18 months of age and on each subsequent birthday.[7] Neonatal screening program in Poland shows that some increased TSH levels (9% versus 3.2%) are from the use of antiseptic iodine and this must be remembered in using the neonatal TSH in

screening for iodine deficiency.[8] Fetal hypothyroidism can occur secondary to treatment of maternal hyperthyroidism or due to congenital thyroid defects and may be cured both by intraamniotic levothyroxine(LT_4) injection 250 or 500 mcg/wk. or maternal administration of the same drug. The transplacental transfer of L-T_4 is demonstrated by the level of free T_3 in fetal blood.[9,10]

REFERENCES

1. McCarrison R. Observations on endemic cretinism, in the Chitral and Gilgit valleys. Lancet 2; 1275-80, 1908.
2. Delange F, Beckers C, Hofer R, Konig MP, Monaco F, Naronne S, Neonatal Screening for congenital hypothyroidism in Europe. Acta Endocr. 90 suppl. 223, 1979.
3. Newborn Committee of the American Thyroid Association. Recommendations for screening programs for congenital hypothyroidism. J Paediatr 89:692-4, 1976.
4. IDD Newsletter, August 1999, P-37.
5. Taher MA, Congenital hypothyroidism. Indian pediatrics 20: 791, 1983.
6. Ishaque AM, Taher MA et al. Neonatal hypothyroidism screening in bangladesh. J Endocr Inv Sep. 1992 Intl. Thy. Symp
7. Klein RZ. Treatment and Follow-up of children with infantile hypothyroidism. p.223-231. In. Medeiros-Neto G, Maciel RMB, Halpern A (eds). Iodine Deficiency Disorders and Congenital Hypothyroidism. Sao Paulo Med. School 1986. Brazil.
8. Oltarzewski M et al. Preliminary evaluation of chamges in blood sport TSH levels based on the neonatal screening program in Poland. IDD Newletter 15(4): 54-56, 1999 (Nov.) quoted from polish J Endocrinol 49 (Suppl 1):63-71, 1998.
9. Nicolini U, Venegoni E, Acaia B et al. Prenatal treatment of fetal hypothyroidism: is there more than one option? Prenat Diagn 16 : 443-448, 1996.
10. Suresh S, Suresh I, Ganesan S. Fetal therapy. In Malhotra N, et al. (eds.) Ultrasound in Obstetrics and Gynecology 3 rd. ed. Jaypee Bros. New Delhi 2001: pp. 174-183.

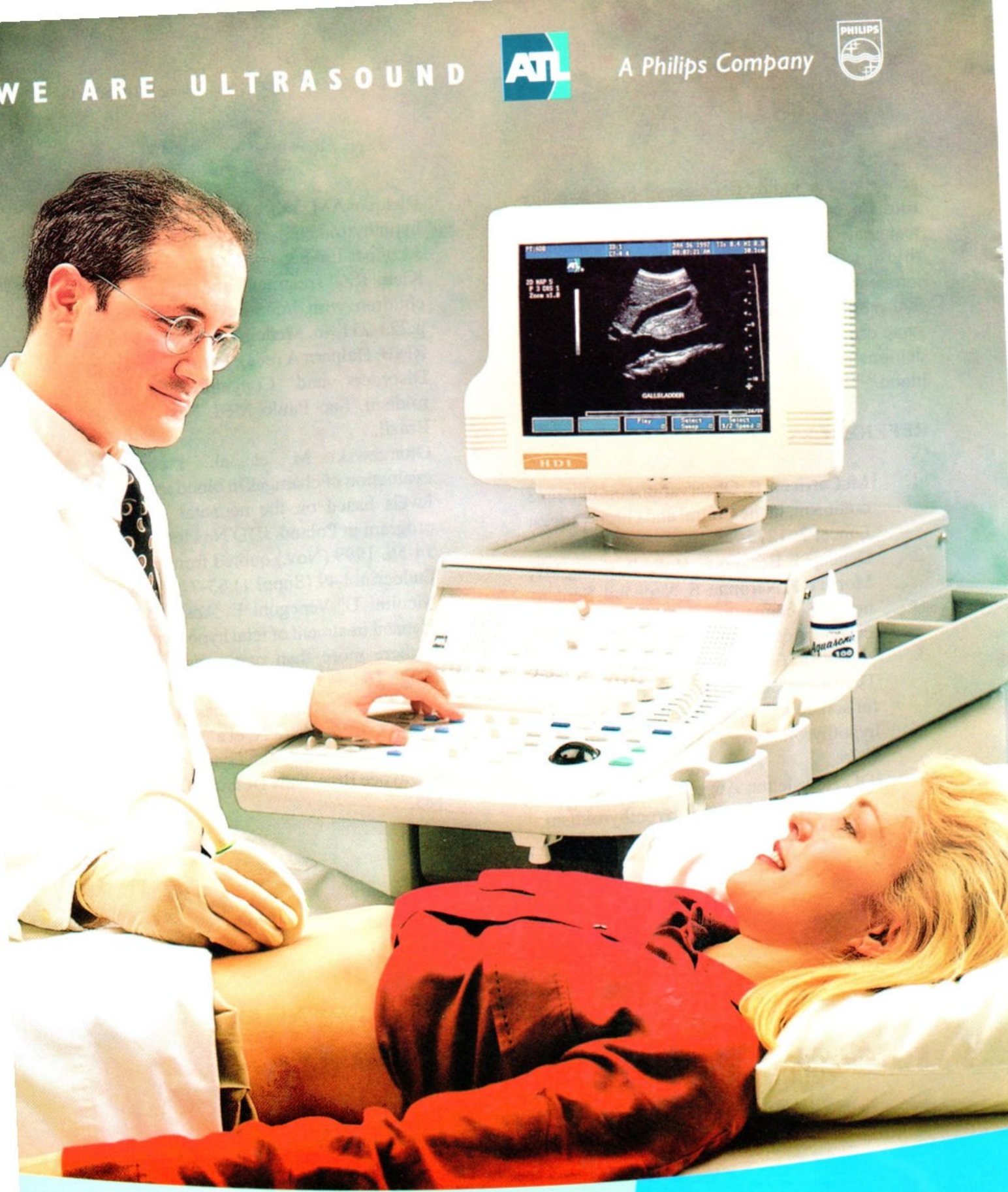

FOR MORE INFORMATION PLEASE CONTACT

PHILIPS MEDICAL SYSTEMS

- TEL. 745-4090 Ext. 3332
- FAX. 398-0792

Philips Electronics (Thailand) Ltd.
209/2 Sanpavuth Road, Bangna, Bangkok 10260

ฆพ. 78/2542

PHILIPS

Let's make things better.

A RETROSPECTIVE STUDY ON POST- OPERATIVE THYROID REMNANT ABLATION IN DIFFERENTIATED THYROID CANCER BY I-131: COMPARISON BETWEEN SUCCESS OF LOW AND HIGH DOSE.

ISLAM S[1], CHAIWATANARAT T[2], POSHYACHINDA M[2], KANUANGNITE K[2].

ABSTRACT

The first and most important step in the management of differentiated thyroid carcinoma is to reduce the chance of recurrence and death. I-131 ablation represents the most specific anti-neoplastic measures in differentiated thyroid cancer. Ablation of thyroid tissue remnant with radioactive iodine (I-131) reduces the risk of recurrence and increases the survival rate.

We studied retrospectively thyroid remnant ablation with low and high dose of I-131 and compare their success. Total 54 patients of low-dose group treated with 20-50 mCi of I-131 and 159 patients of high dose group treated with 100 mCi of I-131 were included in this study. After first dose both group shows variable success (33% versus 62% low dose versus high dose respectively) but nearly similar success in both groups after second dose (81% versus 77% respectively).

From our study it can be concluded that the use of two low doses at 6-12 months interval could be an acceptable and effective method to ablate post-operative thyroid remnant, particularly the young subjects or in the situation of limited hospital bed.

Besides minimizing the whole body and gonadal irradiation exposure, the advantages are more convenience and reduce the expenses with a dose that can be given as an outpatient. In spite of all advantages the disadvantages are that about half of the patients will require more than one dose to ablate and delay in achieving complete ablation.

INTRODUCTION

The First and most important step in the post-operative management of patient with differentiated thyroid cancer is to analyze the factors that affect the risk of recurrence and death.

Post-operative thyroid remnant (POTR) of nonmalignant thyroid tissue always presents after surgery. I-131 treatment for post-operative thyroid remnant in differentiated thyroid cancer represents one of the more specific anti-neoplastic measures. I-131 has been used for more than half a century to ablate POTR following surgery. I-131 ablation probably decrease the risk of recurrence by destruction of microscopic metastases which are known to be present in both the opposite thyroid lobe and ipsilateral lymph

[1] Nuclear Medicine center, Chittagong Medical college hospital campus, Chittagong, Bangladesh.
[2] Nuclear Medicine division, Department of Radiology, Faculty of Medicine, Chulalongkorn University, Bangkok, Thailand.

nodes in 90% of patient with papillary thyroid cancer.[1] Upto 60% of all thyroid cancer and 80% of all differentiated thyroid cancer are treatable with I-131, after removal of most of the thyroid tissue with tumor.

Elimination of residual normal thyroid with its relatively high uptake of I-131 should increase uptake of I-131 in metastases by making more I-131 available to them.[2]

Patients with residual normal thyroid often have detectable thyroglobulin (Tg) even when TSH is totally suppressed while those who have undergone successful ablation usually have low or undetectable Tg, so then it become more sensitive in detecting recurrences in the later group.[3]

There is still much controversy regarding the optimal dose of I-131, required to achieve a successful ablation. Dose of 50-150 mCi are now customarily used to ablate thyroid remnant.

Regarding the efficacy of low dose ablation of POTR in patient with differentiated thyroid cancer, a variable success rate has been reported with empirical low dose therapy. The interest in using low dose lies in the prospect of out patient (OPD) treatment, attendant economy and convenience, decreased risk of leukaemogenesis and extra-thyroidal organ damage from lower whole body radiation exposure. These are among theoretical advantage and may be of special concern in young patients with better prognostic value.

MATERIALS AND METHODS

A retrospective study was done on two groups of patients of differentiated thyroid cancer, treated with low and high dose of I-131, who received I-131 ablation dose for POTR ablation at the Nuclear Medicine section of Radiology Department of Chulalongkorn University.

In the first group (group-A) the patients were treated with low-dose (20-50 mCi) of I-131 in the period of 1980-1988 and in the other group (group-B) the patients were treated with 100 mCi in the recent year of 1996-1999.

Patients included in the study were all had biopsy proven well-differentiated thyroid carcinoma, had history of total/subtotal or at least partial thyroidectomy, treated with I-131 for POTR ablation and had at least 12 months follow-up after ablation.

Patients excluded from the study are those who had inoperable local disease, loco-regional recurrence on presentation, histologic type other than papillary and follicular and those who had history of external radiation. Patients having distant metastases were also excluded but patient with capsular invasion and local lymph-node involvement were included and only one patient with mediastinal mass was included in the low dose group.

All patients performed I-131 whole body imaging after surgery to look for post-operative thyroid remnants (POTR) and metastases, about 6-8 weeks following surgery. This period allows time for the patient to recover from surgery, establishment of vascularity to the site of operation and for circulating T4 to fall to undetectable level and for any stable iodine used in the setting of surgery to be utilized or excreted. I-131 neck and whole body imaging was performed 48 hours after administration of a diagnostic dose (1-2 mCi) of I-131 using Gamma camera or rectilinear scanner. Post therapy scan were done usually on the 2^{nd} to 4^{th} day for low dose group and on the 5^{th} -7^{th} day on the high dose group.

The criteria for complete ablation considered in this study were the absence of any

visible I-131 concentrating tissue on whole body scan with serum Tg of less than 10 ng/ml, after oral thyroxin was taken out from the maintenance doses.

A few days after I-131 ablation dose, patients were started on thyroxin which was taken until 6 week before the next follow up, when T3 will be started for another 4 weeks then no supplement for the last 2 weeks before performing the follow up scan. Patients were then advised to come after 6 months for follow up I-131 whole body scan and serum TSH, T4 and TG levels. Occasionally in few cases Tl-201 scan, 99mTc-MIBI scan, CT scan and CXR were done when Tg level and I-131 TBS were not correlating clinically.

Chi-square test was used to compare success rate of ablation in two groups.

RESULTS

Characteristics of subjects included into this study is presented in table 1. In group-A (low-dose group), total 54 patients were included, with the age range of 8-68 years, 13 male and 41 female, with histopathologic type of 19 papillary, 24 follicular, and 11 mixed cell type. Among these patients 34 had near total thyroidectomy (NTT), 16 had subtotal thyroidectomy (STT) and 4 had partial thyroidectomy, 14 patients had local lymph node metastases. Duration of follow-up ranges from 12 months to 16 years.

In group-B (high-dose group), total 159 patients were included, with age range of 17-84 years, 18 male and 141 female, with histopathologic type of 106 papillary, 29 follicular and 24 mixed cell type. All these patients have NTT and reported no local or distant metastases. Duration of follow-up ranges from 12 to 30 months.

There is marked difference in successful ablation of two groups after 1st dose (Table 4). On low dose group shows only 33.3% ablation success but in high dose group shows about 62.3% of ablation success after first dose which is significantly higher than the low dose group (p value < 0.005). On the contrary, the success rate of ablation in second dose is higher in low-dow dose group than high-dose group (72% vs 42%). After 2nd dose, the ablation success is nearly similar in both group (81.5% Vs 78.0% in low dose and high dose group, respectively, with p value > 0.1). But the average dose given to the patient, after 2nd dose, is significantly different in two groups, 103.07 mCi in low dose group and more than 200 mCi in high dose group.

In our study we tried to give more attention on those patient treated by low dose I-131, to find out the real success and the factors related to success or failure. Like other study on low dose trial, our study also shows good success related to young age and male patients. The patients of papillary cell type treated by low-dose show relatively less success (16%) after the 1st dose but significant success (90%) after the 2nd dose. In case of follicular cell type shows 41% success after the 1st dose and about 80% after 2nd dose but the success in mixed variety is relatively higher (45%) after the 1st dose but relatively lower (72%) after the 2nd dose (table 5).

In our study we have 14 patients with local (cervical) lymph node involvement on initial diagnosis and one of the patients had suspected mediastinal metastases. Out of these 14 patients, one patient was completely ablated by single dose (50mCi), showing no recurrence and 11 patients were ablated by two dose. Two patients need more than two doses.

Table 1. Details patient's characteristics

Patient's Profile	Treated by 20-50mCi (Group-A)	Treated by 100mCi. (Group-B)
Total patients :	54	159
Age range (years) :	8-68	17-89
< 40 years	36	88
> 40 years	18	71
Sex :		
Male	13 (24%)	18 (11.6%)
Female	41 (75.9%)	141 (88.4%)
Histopathologic types :		
Papillary	19 (35.18%)	106 (66.67%)
Follicular	24 (44.44%)	29 (18.23%)
Mixed (P+F)	11 (20.37%)	24 (15.10%)

Table 2 and 3 show variation in success according to the different patient characteristics.

Table 2. Status of patients treated by low dose of I-131

	Single Dose	Two Doses	> Two Doses
Total patients :	18	26	10
Age range (years) :	13-53	19-68	8-63
< 40 years	14 (77.8%)	17 (65.4%)	5 (50.0%)
> 40 years	4 (22.2%)	9 (34.6%)	5 (50.0%)
Sex :			
Male	5 (27.7%)	7 (27.0%)	1 (10.0%)
Female	13 (72.2%)	19 (73.0%)	9 (90.0%)
Histopathologic types :			
Papillary	3 (16.7%)	14 (53.8%)	2 (20.0%)
Follicular	10 (55.5%)	9 (34.6%)	5 (50.0%)
Mixed (P+F)	5 (27.8%)	3 (11.5%)	3 (30.0%)
Average Total Dose (mCi) ±	43.63	103.07	-
SD	±10.45	±24.78	
Recurrent	3 (16.6%)	8 (30.7%)	4 (40.0%)

Table 3. Status of patients treated by high dose of I-131

	Single Dose	Two Doses	> Two Doses
Total patients :	99	25	35
Age range (years) :	17-68	21-75	20-84
< 40 years	44 (44.4%)	13 (52.0%)	18 (52.4%)
> 40 years	55 (55.6%)	12 (48.0%)	17 (48.6%)
Sex :			
Male	11 (11.1%)	3 (12.0%)	3 (8.5%)
Female	88 (88.9%)	22 (18.0%)	32 (91.5%)
Histopathologic types :			
Papillary (total 106)	69 (69.7%)	15 (60.0%)	22 (62.9%)
Follicular	10 (55.5%)	9 (34.6%)	5 (50.0%)
Mixed (P+F) (total 24)	5 (27.8%)	3 (11.5%)	3 (30.0%)
Surgery :			
NTT	99 (100.0%)	25 (100.0%)	35 (100.0%)
STT	-	-	-
Partial thyroidectomy	-	-	-
Total Dose (mCi)	100	200	300

Table 4. Comparison of success of ablation between two groups of patients treated by I-131

Dose group	1st Dose ablation	2st Dose ablation	1st + 2stDose ablation	The rest of the patients
20-50 mCi (Group-A)	18/54 (33.3%)	26/36 (72.2%)	44/54 (81.5%)	10/54 (18.5%)
100mCi (Group-B)	99/159 (62.3%)	25/60 (41.7%)	124/159 (78.0%)	35/159 (22.0%)
P value	< 0.005		> 0.1	

Table 5. Comparison of success of ablation in different cell types between low-dose (A) and high-dose (B) groups.

Cell type	Patients' group	1st Dose ablation	2nd Dose ablation	1st + 2nd Dose ablation
Papillary	A (n = 19)	15.9 %	87.5 %	89.8 %
	B (n = 106)	65.0 %	40.5 %	79.2 %
Follicular	A (n = 24)	41.7 %	64.0 %	79.0 %
	B (n = 29)	62.0 %	45.4 %	79.3 %
Mixed	A (n = 11)	45.4 %	50.0 %	72.7 %
	B (n = 24)	50.0 %	46.7 %	70.8 %

DISCUSSION

Despite many controversies, I-131 has been used for nearly 50 years to ablate POTR as fundamental steps in the management of differentiated thyroid carcinoma to prevent risk of recurrence and death. Arguments in favor of I-131 ablation includes the existent, though low, mortality from differentiated cancer and it's known response to I-131,[4] the multicentric nature of the tumour,[5] the known recurrence in remaining normal thyroid[6] and the known association between differentiated and anaplastic cancer,[7] possibility of occult cervical lymph node metastases showing up after ablation,[8,9] and facilitation of follow up assessment[4,10] and improved survival in certain subsets.[11,12] Therefore thyroid remnant ablation should lead to low recurrence rate and improved chance of survival in the majority of patients.[13]

Because of wide variation in uptake and size of residual thyroid, no amount of radioiodine can ensure complete ablation. It appears that 30 mCi of I-131 can completely destroy the thyroid remnant in some patients while 150 mCi may not be sufficient in others. The radiation dose delivered to the thyroid remnant depends not only the number of mCi administration but also depends on the size of the remnant, the thyroid uptake and the effective half-life (T1/2 eff) of I-131 of the remnant.[2]

Before I-131 administration for whole body imaging, ablation or treatment of thyroid cancer, condition should be optimized so that uptake of I-131 is as high as possible. This will increase effectiveness of treatment, since doubling the uptake is equivalent to giving twice as much I-131.[2]

Differentiated thyroid carcinoma has receptor for TSH, but much less sensitive to being stimulated than normal thyroid follicular cells. Prior to whole body imaging, ablation or therapy, thyroid hormone should be discontinued to induce temporary hypothyroidism. Serum TSH should be determined before imaging or ablation to ensure that TSH is sufficiently elevated.[2]

The second major determinant of radioiodine uptake is the serum inorganic iodine concentration as it competes with I-131 to enter thyroid follicular cells at level of iodine trapping. An increase in number of inorganic iodine in blood decreases the uptake of radioiodine.

The most appropriate and effective dose

of I-131 for successful ablation of POTR is controversial. In different literatures variable dose recommendation from different authorities, ranging from 20-250 mCi, have been reported.[13-17] It was believed for a long time that higher initial I-131 doses are more effective in achieving complete ablation with a single dose.

There are some controversies about the appropriate approach, whether patients with POTR should be treated with series of empirical dose of I-131 or whether the dose should be individualized by careful dosimetry after appropriate tracer studies.

Some groups tried to quantitate the activity of iodine necessary to ablate residual thyroid. In delivering 30,000 rads (about 30 mCi), Maxon et al[18] achieved successful ablation in 81% of 70 patients, with no increase in success rate at higher doses.

McCowen et al[19] reported that doses of 80-100 mCi were not more effective than 30 mCi. Other retrospective studies confirmed similar findings.[13,20] In addition, various prospective studies have also shown that low dose I-131 ablation is as effective as high dose in achieving successful ablation by single dose.[16,17,21,22]

In 1995, Chandrsekhar et al reported the ablation rate of 63% at 19,800 cGy and increased to 77.8% at 31,372 cGy with no further increase ablation even at 130,200 cGy. Since thyroid malignancy is heterogenous in nature, it may harbour variable populations of relatively radiosensitive and radio-resistant cells which may explain the observation. Most probable the radiosensitive cells are killed first and leave the relatively radio-resistant cells in situ with sublethal damage. These sub-lethally damaged cells may behave in two ways: part of them becomes more susceptible to subsequent destruction due to a higher radiation absorbed dose and the remaining cells evolve in a true radio-resistant population. So even we increase the administered dose to the thyroid gland while the radio-sensitive cell population is constant, the radiation absorbed dose beyond 30,000 cGy is only going to increase the undue whole body radiation to the individual.

In our study we found lower success rate of ablation (33%) in low-dose group and relatively high success rate (62%) in high-dose group after the first dose. Interestingly after the second dose, the success ablation in both groups are similar (81% vs. 78%). The likely explanation for slightly lower success ablation after second dose in high-dose group as compared to low-dose group is that higher administered activity of I-131 yields a grater radiation dose which may produce changes in thyrocyte that can grossly shorten effective half-life and reduced the actual radiation dose to thyroid in subsequent therapy.

Our results show that by using low dose regimen we can reduce the average total I-131 dose to nearly half of high dose, therefore radiation exposure to the patient can be significantly reduced. Our results show that repeated low dose administration for thyroid remnant ablation is very useful and effective, where success rate is nearly similar to higher dose. It is believed that repeated low dose exposures allow the tissue repair mechanism to proceed in the interim period and it may cause less biological damage than the same total dose delivered to the patient as a single dose.[2]

Different studies discussed here showed some patients whose scan were borderlines at 6 months interval, become negative after observation for 12-18 months. Therefore it is suggested that a minimal or borderline positive scan at 6 months after first therapy dose is an indication of further observation rather than immediate further ablation dose. But patient with persistently

positive scan after two successive low-dose, the subsequent dose should be increased.

Serum thyroglobin (Tg) is currently the most accurate way to detect recurrent thyroid cancer whether or not the patient is taking thyroid hormone. Most well-differentiated thyroid cancers but not the medullary or anaplastic cancers secrete Tg even if they do not concentrate radio-iodine. Under appropriate circumstances, serum Tg can be used as a tumour marker for persistent or recurrent well differentiated thyroid cancers.[24-30] Though in most of the patients of our study Tg correlated but few cases show raised Tg, without any detectable residual or metastatic focus in TBS. In those cases also Tl-201, MIBI or CT-scan were done and shows no detectable tissue or metastases. Interestingly most of the patient in this group shows decreased Tg value in subsequent follow-up in 12-18 Months without any treatment.

According to our study both papillary and follicular cell types show lower successful thyroid ablation in low-dose group as compared to high-dose group.

The advantages of low dose include avoidance of undue high radiation dose to some patients, decrease incidence of both early and late complications of I-131 therapy. Moreover low dose ablation is convenient and more economy since some patients can be treated as outpatients of which it is helpful for hospitals with limited beds.

In spite of all benefits of low dose, it's disadvantages should be considered as more than half of the patients required repeated dose, need longer time to achieve ablation and unrecognized metastases may be inadequately irradiated.

CONCLUSION

Considering all merits and demerits of low dose ablation it would be concluded that with empirical selection of suitable low-dose, patient selection, adequate patient's preparation and elimination of some factors to optimize the uptake of radioiodine will increase the effectiveness of low-dose ablation. We can therefore advocate the low dose as an alternative way for conservative and economic approach to thyroid remnant ablation in differentiated thyroid cancer. High dose should be reserved for cases with higher risk of recurrence and for treatment of metastases.

ACKNOWLEDGEMENT

I like to express my honour and gratitude to my supervisor Dr. Vacharee Buachum who always inspired me to do some research work during fellowship course. I am very grateful to Dr.Anchali Krishnachinda, who first inspired me to start such a research work. I like to thanks all medical staffs and resident doctors who always co-operate me in collecting patient's data. I like to thanks Librarian of Faculty of Medicine, Chulalongkorn University for supplying me with the reference journals and books. Finally, I like to thanks BAEC for nominating me for the Fellowship course and IAEA for arranging and supporting such a good fellowship course.

REFERRENCES

1. Hurley JR, Becker DV. The use of radio-iodine in the management of thyroid cancer. In: Freeman LM, Weissman HS (eds). Nuclear Medicine Annual. New york: Raven press, 1983:329-84.
2. Hurley JR, Becker DV. Treatment of thyroid cancer with Radio-iodine. In: Sandler MP, Patton JA, et al. (eds). Diagnostic Nuclear Medicine 3rd Edition Vo. 2, Baltimore: Williams & Wilkins, 1996: 959-89.

3. Pacini F, Lari R, Mazzeo S, Grasso L, Tuddei D, Pinchera A. Diagnostic value of a single serum thyroglobin on and off thyroid suppressive therapy in the follow-up of patients with differentiated thyroid cancer. Clin Endocrinol 1985;23:405-11.
4. Pochin EE. Radio-iodine therapy of thyroid cancer. Semin Nucl Med 1971;1: 503-15.
5. Black BM, Kirk TA, Woolner LB. Multi-centricity of papillary adenocarcinoma of the thyroid, influence of treatment. J Clin Endocrinol Metab 1960;22:130-5.
6. Mazzaferri EL and Young RL. Papillary thyroid cancer. A 10 year follow-up. Am J Med 1981;70:511.
7. Leeper RD. The effect of therapy on survival of patients with metastatic papillary or follicular thyroid carcinoma. J Clin Endocrinol Metab 1973;36,1143-52.
8. Henk JM, Kirman S and Owen GM. Whole body scanning of I-131 therapy in the management of thyroid carcinoma. Br J Radio 1972;45:369-76.
9. Coakley Aj, Page CJ and Croft D. Scanning dose and detection of thyroid metastases (letter). J Nucl Med 1980;21: 803.
10. Beierwaltes WH. The treatment of thyroid carcinoma with radioactive iodine. Semi Nucl Med 1978;8:79-94.
11. Varma VM, Beierwaltes WH, Noafl MM, Nishiyama RH and Kopp JE. Treatment of thyroid cancer; death rate after surgery and after surgery followed by sodium I-131. JAMA 1970;214:1437-42.
12. Mazzaferri EL and Jhiang SM. Long term impact of initial surgical and medical therapy on papillary and follicular thyroid cancer. Am J Med 1994;97:418-28.
13. Degroot LJ, Reilly M. Comparison of 30-50 mCi doses for I-131 for thyroid ablation. Ann Intern med 1982;12:51-3.
14. Beierwaltes WH, Rabbani R, Dmuchowski C, Lloyd RV, Eyre P, Malleltte S. An analysis of "ablation of thyroid remnants" with I-131 in 511 patients from 1947-1984: Experience at University of Michigan. J Nucl Med 1984;25: 1287-93.
15. Sammuel AM, Rajashekharrao B. Radio-iodine therapy for well differentiated thyroid cancer: A quantitative dosimetric evaluation for remnant thyroid ablation after surgery. J Nucl Med 1994;35:1944-50.
16. Cruetzig H. high or low dose radio-iodine ablation of thyroid remnants. Eur J Nucl Med 1987;12:500-2.
17. Johansen K, Woodhouse NJY, Odugbsan O. Comparison of 1073-3700 MBq I-131 in post operative ablation of residual thyroid tissue in patients with differentiated thyroid cancer. J Nucl Med 1991;32: 252-4.
18. Maxon HR, thomas SR, Hertzberg VS, Boehinger A. Relation between effective radiation dose and outcome of radio-iodine therapy for thyroid cancer. N Eng J Med 1983;309:937-41.
19. McCowen Kd, Adler RA, Ghaed N, Verdon T, Hofeldt FD. Low dose radio-iodine thyroid ablation in post surgical patients with thyroid cancer. Am J Med 1976;61:52-8.
20. Ramacciotti C, Pretorius HT, Line BR, Goldman JM and Robbins J. Ablation of non-malignant thyroid remnants with low doses of radio-active iodine: concise communication. J Nucl Med 1982;23:483-9.
21. Leung SF, Law MWM and Ho SKW. Efficacy of low dose I-131 ablation of post-operative thyroid remnants: a study of 69 cases. Br J Radiol 1992;65:905-9

22. Bal CS, Padhy AK, Jana S, Basu AK. Comparison of low and high dose I-131 ablation of remnant in differentiated thyroid cancer patients. In: Rao Rs Deo MG Sanghvi LD (eds). Proceedings of the XVI international cancer congress; 1994, Oct 30-Nov 5; New Delhi, 1994:1059-63.
23. Chandrasekhar Bal, Ajit K Padhy, Gauri S. Pant, A K Basu. Prospective Randomized Clinical Trial to evaluate the Optimal Dose of I-131 for Remanant Ablation in Patients with Differentiated Thyroid Carcinoma. Cancer 1996;77: 2574-80.
24. Ryff-De-Leche A, StaubJ-J, Kohler-Faden R, Muller-Brand J, Heitz PU. Thyroglobin production by malignant thyroid tumours: an immunocytochemical and radio-immunoassay study. Cancer 1986;57:1145-53.
25. Van Herle AJ, Vassart G, Dumont JE. Control of thyroglobulin synthesis and secretion (First of two parts). N Engl J Med 1979;301:239-49, Control of thyroglobulin synthesis and secretion (second of two parts). 307-14.
26. Refetoff S and Lever EG. The value of serum thyroglobulin measurement in linical practice. JAMA 1983;250:2352-7.
27. Ashcraft MW and Van Herle AJ. The comparative value of serum thyroglobin measurement and iodine-131 total body scan in the follow up study of patients with treated differentiated thyroid cancer. Am J Med 1981;71:806-14.
28. Girelli ME, Busnardo B, Amerio R, Casara D, Betterle C, Piccolo M. Critical evaluation of serum thyroglobulin (Tg) levels during thyroid hormone suppression therapy versus Tg level after hormone withdrawal and total body scan: results in 291 patient with thyroid cancer. Eur J Nucl Med 1986;11:333-5.
29. Ozata M, Suzuki S, Miyamoto T, Liu RT, Feerro-Renoy F. Degroot LJ. Serum thyroglobulin the follow up of patients with treated differentiated thyroid cancer. J clin Endocrinol metab 1994;79:98-105.
30. Lubin E, Mechilis-frish S, Zatz S, et al. Serum thyroglobulin and I-131 whole body scan in the diagnosis and assessment of treatment for metastatic differentiated thyroid carcinoma. J Nucl Med 1994;35: 4:257-62.

FIBROADENOMATIOD HYPERPLASIA: IMAGING APPEARANCES AND PATHOLOGICAL CORRELATION.

Darunee BOONJUNWETWAT [1] Patcharajiree ARTTHACHINTA [1]
Pichet SAMPATANUKUL [2] Kris CHATAMRA [3]

Fibroadenomatoid hyperplasia is a benign breast lesion with the composite histologic features of a fibroadenoma and fibrocystic changes. This well-described but rare lesion has been referred to previously as fibroadenomatosis, fibroadenomatoid mastopathy or sclerosing lobular hyperplasia.[1-4] There have been reports with 5-11.5% of this changes in the biopsy population.[1,2] The radiographic finding is unique but the natural history and appropriate diagnostic designation were still in question. We report 3 cases of this specific entity, one with unusual presentation of nonpalpable mass in the breast and enlarged right axillary lymph node, and others presenting with solid masses.

CASE REPORT

CASE 1

A 38-year-old woman presented in January 1999 with a palpable lump in her right axilla and tenderness for 2 weeks. There was no abnormal nipple discharge. She had experienced right breast mass 10 years ago and it turned out to be benign mass after surgical removal. Physical examination revealed a 3 cm. well circumscribed mass that was firm and freely mobile in right axilla. The left breast contained nodular area at upper outer quadrant. There was no palpable breast mass bilaterally. Right axillary adenopathy was clinically diagnosed. The patient had been investigated to search for primary lesion within the breast, including mammography, ultrasonography and MRI. Mammography showed ill-defined lobulated mass located at the upper outer quadrant of left breast (Fig. 1A). As correlated with ultrasonograms, it revealed a lobulated-shaped hypoechoic lesion, about 1.8x0.5 cm. in size. No architectural distortion or microcalcification was observed. There were multiple enlarged dense lymph nodes in right axilla, ranged from 2.6-1.2 cm. in diameter, with increased vascular flow on doppler scan. MRI of the breasts was then performed with contrast enhancement and dynamic study. The study showed an area of low signal intensity on T1WI, high signal intensity on T2WI, STIR and SpGr (Fig. 1B) and homogeneous enhancement after Gd DTPA injection at left upper outer quadrant. The enhancement kinetic showed a slow enhancement mass with a linear time course of the time/signal intensity curve (Fig. 1C) Multiple enlarged right axillary lymph nodes were seen. No definite mass or parenchymal distortion of the right breast was visualized. The patient was then admitted with initial diagnosis of right axillary adenopathy.

After excisional biopsy of the left breast mass under stereotactic needle localization and fine needle aspiration of the right axillary lymph nodes were performed. Microscopically, the mass-like lesion shows ill-defined margin blending with the surrounding breast that elicits fibrocystic change (Fig.1D). No sharp circumscription is appreciated. The stromal proliferation and slit-like

[1] Department of Radiology,Faculty of Medicine, Chulalongkorn University, Bangkok, Thailand
[2] Department of Pathology, Faculty of Medicine, Chulalongkorn University, Bangkok,Thailand
[3] Department of Surgery, Faculty of Medicine, Chulalongkorn University, Bangkok, Thailand

epithelial formations result in a picture reminiscent of fibroadenoma. Fibrohyalinization of stroma is prominent. Lobular architecture maintains in part on the left lower field (Fig.1D). At higher magnification, the lobule undergoes fibrohyalinization and so-called fibroadenomatoid change (Fig. 1E).

CASE 2

A 36-year-old woman was referred for screening mammography in September 1999. She also had pain in her left breast for 3 months but there was no palpable mass on the physical examination. The mammograms showed a small mass with partially obscured margin at upper outer quadrant of left breast (Fig.2A). Bilateral benign-appearing axillary lymph nodes were visualized. The additional sonography reveals a 7 mm. low echoic mass at left upper outer quadrant corresponding with the nodule in mammography. Microlobulation of border of the lesion and minimal posterior enhancement were apparent, being cathegorized as indeterminated lesion (Fig. 2B). Needle localization excisional biopsy of the mass under ultrasound guidance at left upper outer quadrant was then performed (Fig. 2C). Microscopically, the well-defined mass consists of proliferating ducts and myxomatous stroma. Fibroadenomatoid hyperplasia is the pathological diagnosis.

CASE 3

A female patient, 52 years of age, sought medical attention for her postmenopausal hormonal replacement therapy in October 1999. She was then referred for screening mammography. The study showed isodense lobulated mass with indistinct margin at inner middle portion of the right breast, measured about 1.2 cm. in diameter. No microcalcification was seen (Fig. 3A). The additional sonography revealed lobulated low echoic mass with ill-defined margin, measured about 0.8x1.2 cm. in size, at inner middle portion of the right breast (Fig. 3B). Excisional biopsy of the mass for tissue diagnosis was done. The section demonstrates confluent lobules with fibroadenomatoid change (Fig. 3C, D).

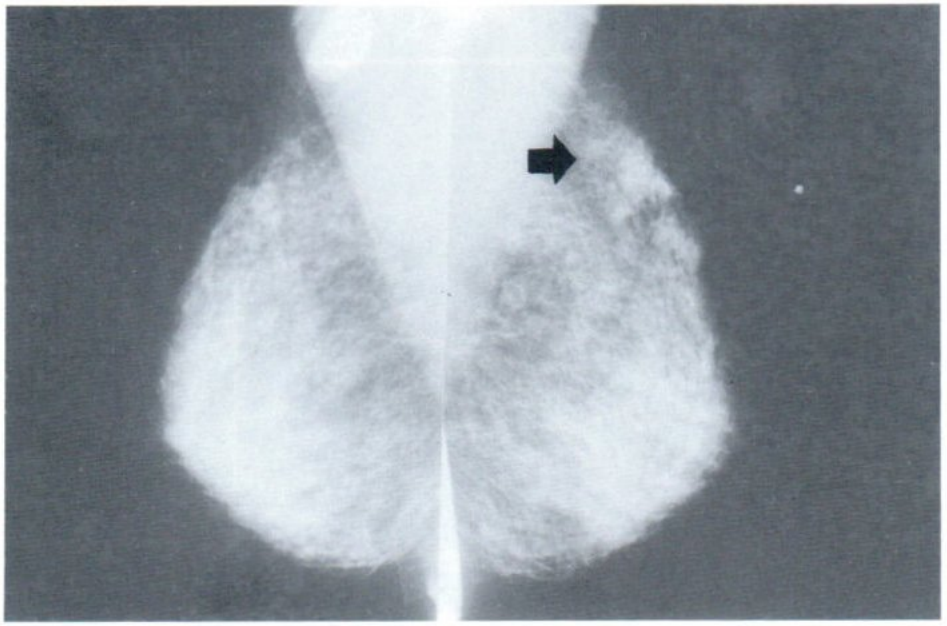

1A

Fig. 1 – 38-year-old woman with fibroadenomatoid change of the left breast and contralateral axillary lymph node hyperplasia

A. Mediolateral mammograms of both breasts show ill-defined lobulated mass at upper outer quadrant of the left breast (arrow). Enlarged right axillary lymph nodes are also demonstrated.

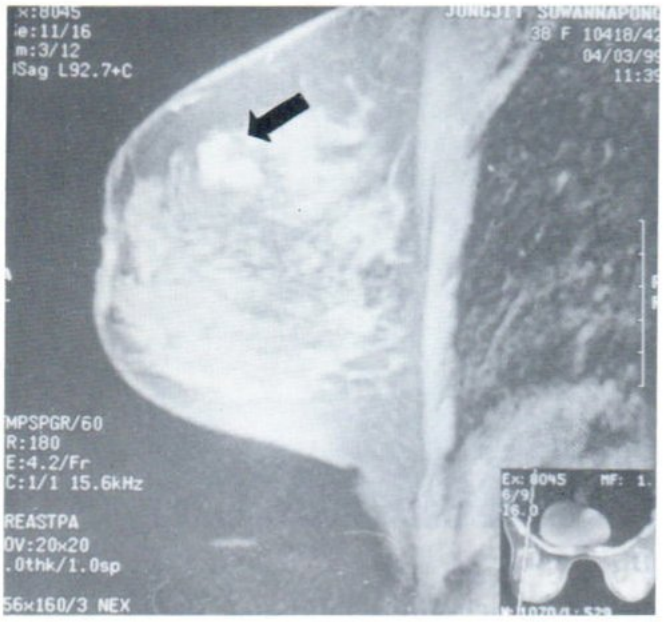

1B

Fig. 1B. Sagittal gadolinium-enhanced MRI image (TR/TE, 180/4.2) of left breast reveals homogeneous enhancement of the lobulated mass at upper outer quadrant of the left breast (arrow).

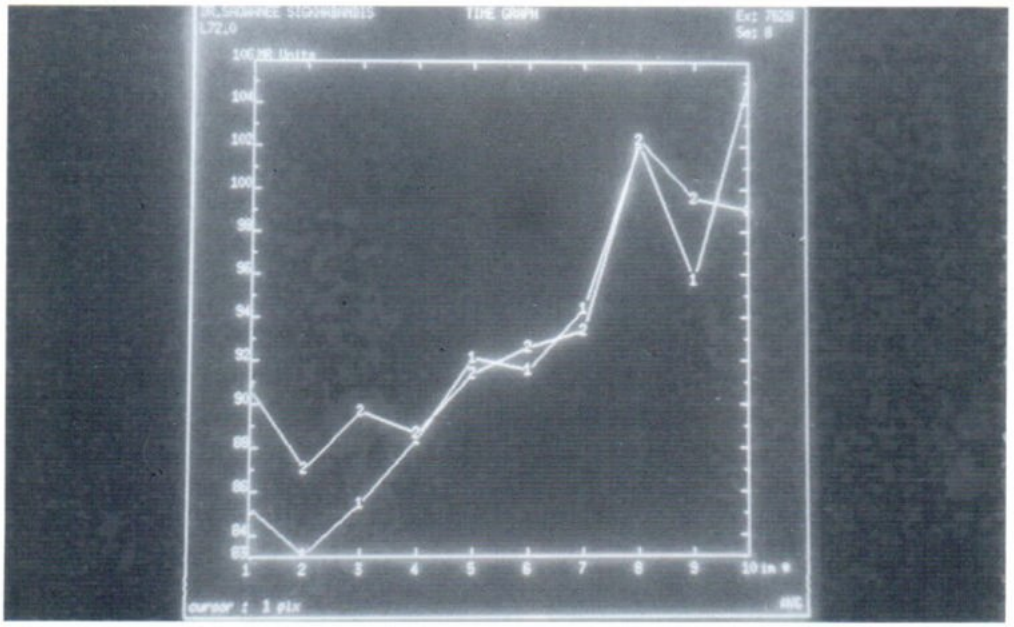

1C

Fig. 1C. Time/ signal intensity curve shows slow enhancement of the lesion with a linear time course.

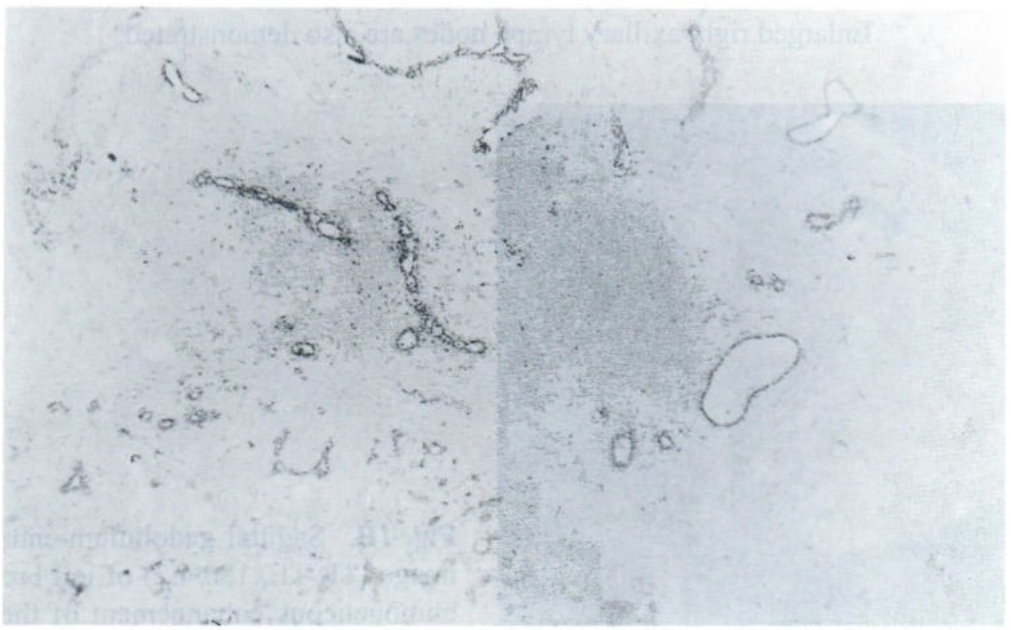

1D

Fig. 1D. Microscopic demonstration of the border of the mass-like lesion. Note the margin blends with the surrounding breast and a lobular architecture maintains (H&E x 40).

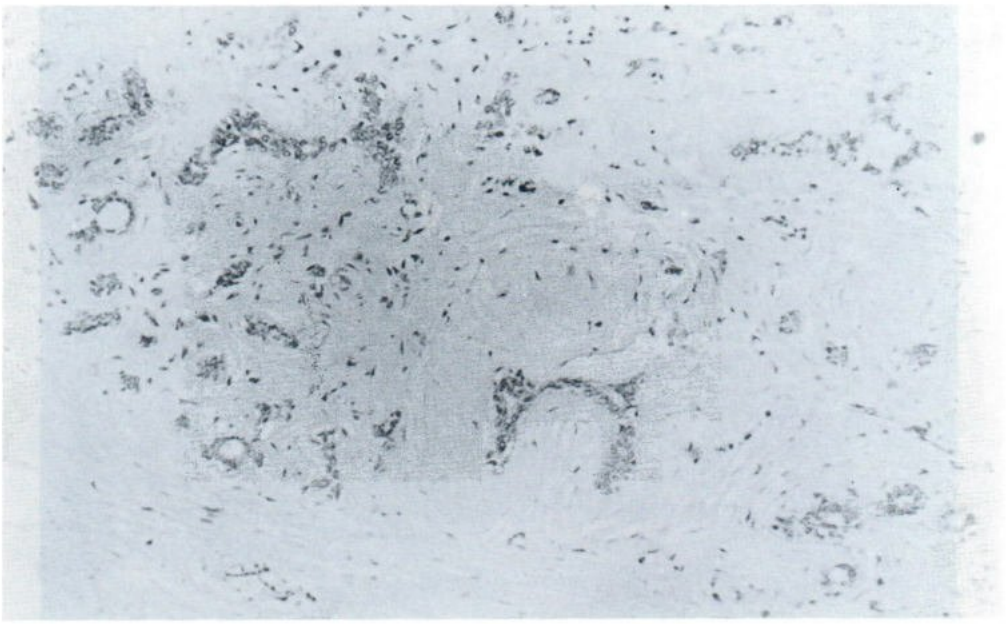

1E

Fig. 1E. The lobule elicits fibroadenomatoid change (H&E x 100).

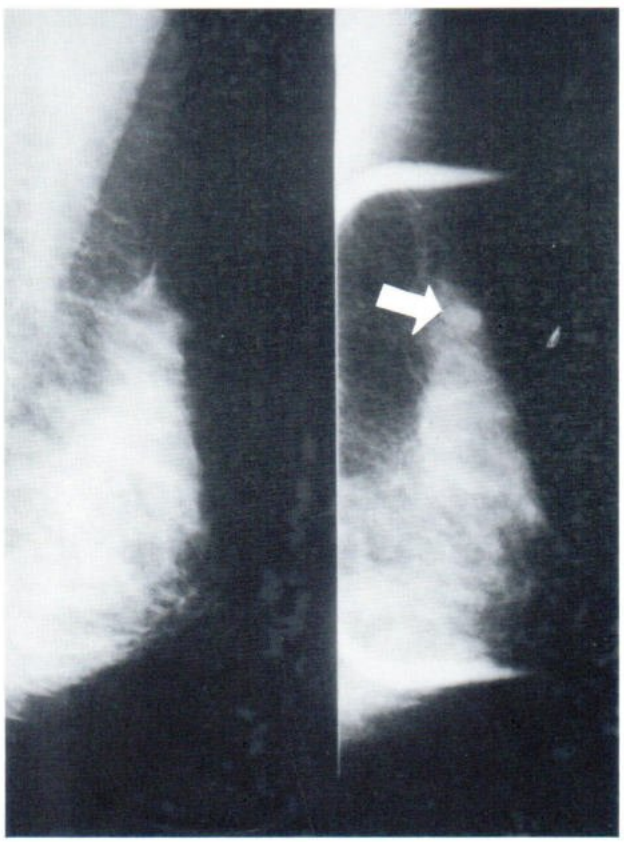

2A

Fig. 2 Breast screening examination of 36-year-old woman

A. Mediolateral mammogram and spot compression views reveal a small-circumscribed lesion partially obscured by breast tissue at upper outer quadrant of the left breast (arrow).

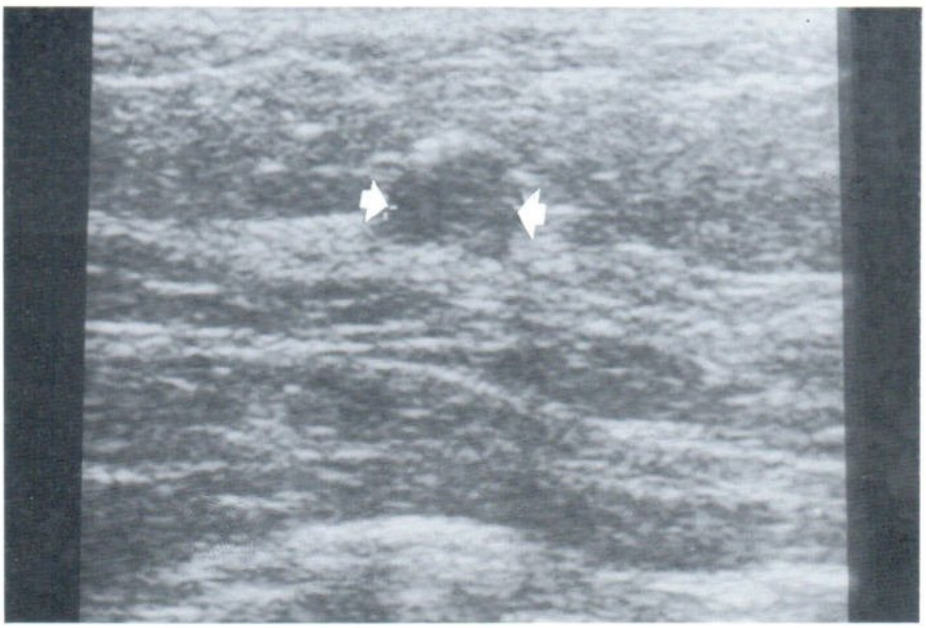

2B

Fig. 2B. The corresponding sonography of the lesion demonstrates a 7 mm. low echoic mass (arrowheads). Also noted is microlobulated border of the lesion and minimal posterior enhancement.

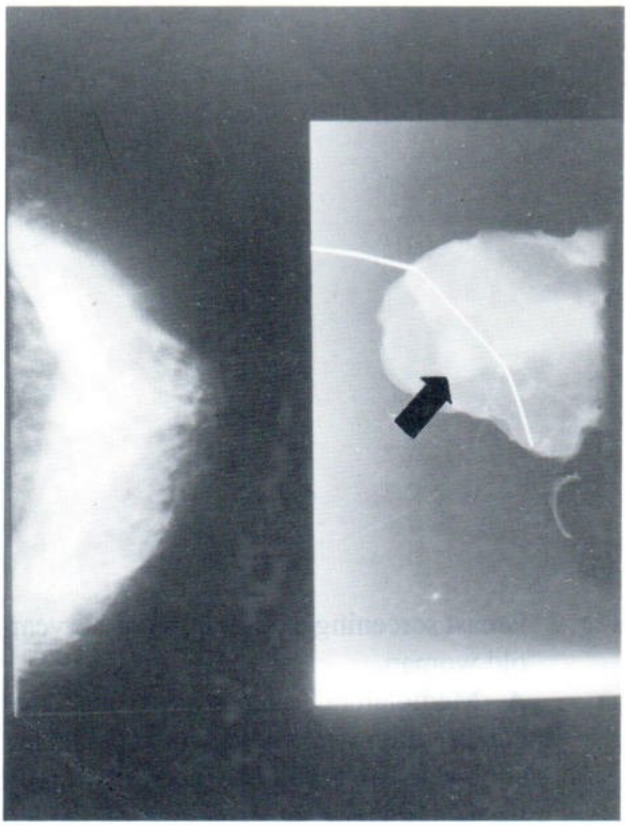

2C

Fig. 2C. The lesion (arrow) was excised after needle localization under ultrasound guidance.

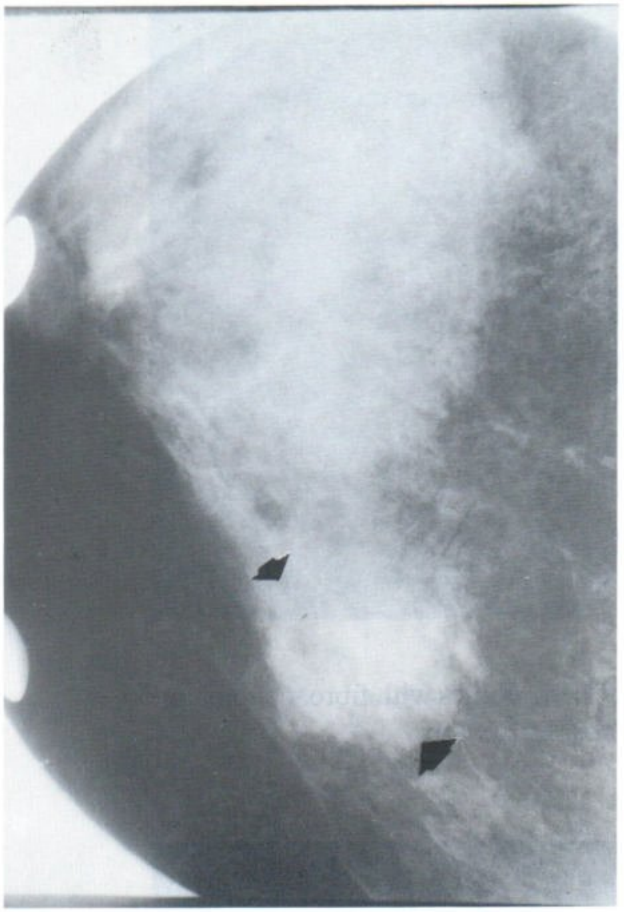

3A

3B

Fig. 3 – 52-year-old woman with fibroadenomatoid hyperplasia of the right breast mass

A. Spot compression craniocaudal mammogram of the mass at inner middle portion of the right breast shows an isodense lobulated mass with ill-defined margin (arrowheads).

Fig. 3B. The sonography also shows lobulated contour of the low echoic mass (arrowheads).

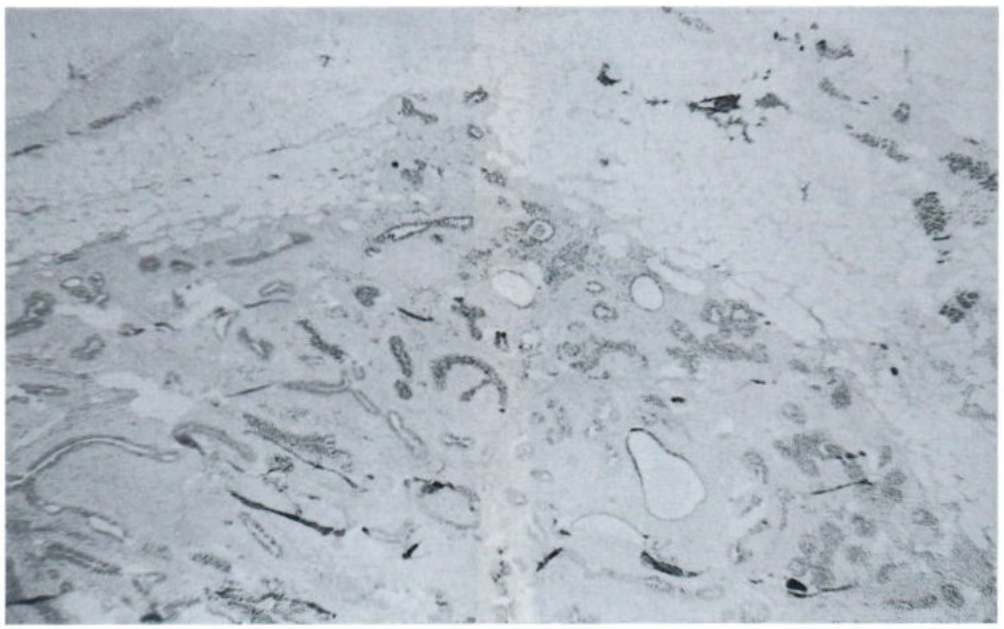

3C

Fig. 3C. Microscopic demonstration of confluent lobules with fibroadenomatoid change. Note the spiculated outline (H&E x 20).

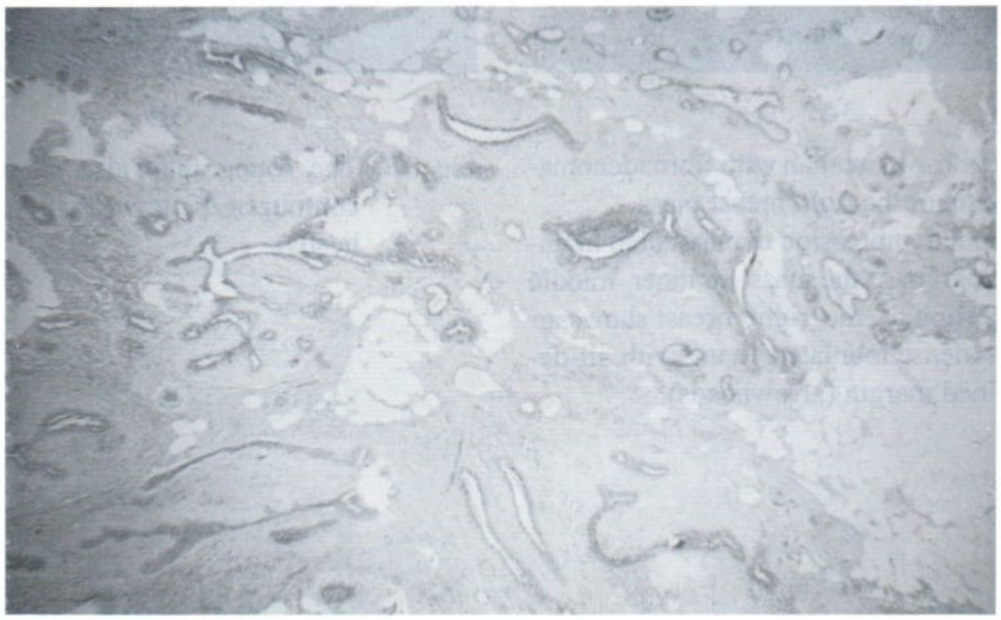

3D

Fig. 3D. The breast lobules with fibroadenomatoid change merge with each other and leave some adipose tissue at the interface areas (H&E x 20).

DISCUSSION

Fibroadenomatoid hyperplasia is a rare benign breast lesion that was previously described in many pathologic and radiologic reports. Semb first has used the term fibroadenomatosis in 1928 for the process that may have preceded a circumscribed fibroadenoma.[5] It has been defined by Cole et.al. in 1978 as mixed lesions having both fibrocystic and fibroadenomatous elements.[6] This lesion is distinct from the typical well-circumscribed fibroadenoma that may have fibrocystic change. The peak age incidence is 30-34 years, which is intermediate to both fibroadenoma (20-29 years) and fibrocystic disease (40-44 years) as well as its histologic appearance. The incidence is between 5-11.5% in benign breast lesions biopsy series with no significant difference in Japanese and American women.[1,2] This lesion has also been reported in a 69-year-old male patient receiving diuretics (spironolactone) for congestive heart failure treatment as multiple fibroadenoma-like nodules.[7] No association with the oral contraceptive pills or breast cancer is presented.

Pathologically, this lesion is characterized by diffusely fibrous and nodular processes rather than a discrete circumscribed mass the same as fibroadenoma, but microscopically fibroadenomatoid foci are intermingled with dilated ducts, epitheliosis and adenosis. It is suggested that fibroadenomatoid hyperplasia is yet another pattern in the complex morphologic spectrum known as benign proliferative breast disease.[1] It may represent a morphologic stage in the development of fibroadenoma but it is best to consider fibroadenoma as a completely distinct entity. It is also suggested that the natural history of fibroadenomatoid hyperplasia is parallel to that of fibroadenoma with regression and calcification over time reflecting degenerative process.[8]

As to our knowledge, the mammographic appearance of fibroadenomatoid hyperplasia has not been well documented in the radiology literatures. In 1995, Poulton described 15 patients with this features presenting with 1-8 cm. breast masses and the mammographic findings were well-defined, medium-density mass in about half of the patients (53%).[4] The most common mammographic findings were a well-defined mass or normal findings. Fibroadenomatoid hyperplasia was reported in 1998 by Kamal et.al. as a cause of suspicious microcalcification on mammographic screening in postmenopausal women older than 50 years of age.[8] Sonography cannot differentiate this specific entity from other solid breast lesions. Furthermore, our literature review showed that there was no previous report about MR characteristic of fibroadenomatoid hyperplasia. The breast MR appearance in case 1 was a focal mass with lobulated shape, homogeneous signal intensity, increased signal intensity on T2WI, slowly enhancement and a linear time-signal intensity curve. These features are indicative of benign lesion commonly found in fibroadenoma.[9] In contrary, the invasive breast cancers tend to exhibit irregular or spiculated contour, heterogeneous signal intensity, low signal intensity on T2WI and strong rapid enhancement with a washout time course.[10,11]

In the first case illustrated, the nonpalpable left breast mass was shown mammographically as an ill-defined mass and sonographically as a hypoechoic lesion, 1.8x0.5 cm. in size. This abnormal presentation warranted the biopsy for tissue diagnosis, which led us to the pathologic conclusion of fibroadenomatoid mastopathy of the mass and lymphoid hyperplasia of the lymph nodes. For the second and third cases, the lesions were found from the screening mammography and supplement sonography being a solid mass with lobulated contour and ill-defined margin.

In conclusion, the fibroadenomatoid

hyperplasia that found in our three cases showed the mammographic and ultrasonographic features of a mass with lobulated contour, being classified as category 3 and 4 according to American College of Radiology Breast Imaging Reporting and Data System (ACR BIRADS).[12] As compare to the MRI, the signal intensity and post contrast dynamic study of the lesion in our first case indicated the benign characteristic. Consequently, the fibroadenomatoid hyperplasia is one of the benign lesions that give the imaging features mimic that of malignancy. It is difficult to make the appropriate judgement for doing biopsy or follow up. In our opinion, the breast MRI with dynamic contrast study would help to distinguish benignity from malignancy in the lesion that is indeterminated by mammography and ultrasonography.

REFERENCES

1. Hanson CA, Snover DC, Dehner LP. Fibroadenomatosis (fibroadenomatoid mastopathy): a benign breast lesion with composite pathologic features. Pathology 1987;19:393-396
2. Schuerch C, Rosen PP, Hirota T, et al. A pathologic study of benign breast diseases in Tokyo and New York. Cancer 1982;50: 1899-1903
3. Kovi J, Chu HB, Leffall LD. Sclerosing lobular hyperplasia manifesting as a palpable mass of the breast in young black woman. Hum Pathol 1984;15:336-340
4. Poulton TB, de Paredes ES, Baldwin M. Sclerosing lobular hyperplasia of the breast: imaging features in 15 cases. AJR 1995;165:291-294
5. Semb C. Pathologico-anatomical and clinical investigations of fibroadenomatosis cystica mammae and its relationship to other pathological conditions in the mamma, especially cancer. Acta Chir Scand 1928;64 (Suppl 10):1-482
6. Cole P, Elwood JM, Kaplan SD. Incidence rates and risk factors of benign breast neoplasms. Am J Epidemiol 1978;108: 112-120
7. Nielsen BB. Fibroadenomatoid hyperplasia of the male breast. Am J Surg Pathol 1990;14(8):774-777
8. Kamal M,Evans AJ,Denley H, Pinder SE, Ellis IO. Fibroadenomatoid hyperplasia: a cause of suspicious microcalcification on mammographic screening. AJR 1998;171: 1331-1334
9. Brinck V., Fischer V, Kanablowska M., Schauer A., Grabbe E. The variability of fibroadenoma in contrast-enhanced dynamic MR mammography. AJR 1997; 168:1331-1334
10. Kuhl CK., Micleerek P, Klaschik S, et al. Are signal time course data useful for differential diagnosis of enhancing lesion in dynamic breast MR imaging? Radiology 1999;211:101-110
11. Kuhl CK, Mielcarek P, Klaschik S, Pabos E, Schild H. Are T2 weighted pulse sequences helpful to assist differential diagnosis of enhancing lesions in dynamic breast MRI? J Magn. Reson Imaging 1999; 9:187-196
12. Feig SA. Principles and Practice of Breast Imaging. Seminar in Breast Disease 1999; 1:3-16

COST - EFFECTIVENESS ANALYSIS OF RADIOIMMUNOASSAY AND IMMUNOTURBIDIMETRIC TESTS FOR MICROALBUMINURIA

Wiwanitkit V.[1]

Objective: To perform cost - effectiveness analysis of radioimmunoassay and immunoturbidimetric tests as diagnostic markers in detection for microalbuminuria
Setting : King Chulalongkorn Memorial Hospital
Design : Retrospective study
Subjects : data about cost and effectiveness of two categories for detecion for acute pancreatitis performing by radioimmunoassay and immunoturbidimetric tests
Methods : Review relating literature then economical-based cost-effective analysis was performed.
Results : Cost-effectiveness of radioimmunoassay test was 267.86 baht /diagnosis and of immunoturbidimetric test was 80.65 baht/diagnosis
Conclusion: immunoturbidimetric was more cost-effective method than radioimmunoassay for detection for microalbuminuria

KEY WORDS : cost-effectiveness, microalbuminuria

Microalbuminuria (MAU) has been recognized as an independent and reliable predictor for future development of overt proteinuria in diabetic patients.[1] It represents the condition in which abnormal micro quantities of albumin, not detectable by simple urine dipstick, are excreted into the urine. It is associated with a high morbi-dity and mortality form of diabetic nephropathy[2-5] as well as coronary artery diseases.[1] Furthermore, there have been many reports on the association between microalbuminuria and an increasing incidence of diabetic retinopathy.[1]

Therefore, microalbuminuria is an important biomarker for monitoring complications of diabetic patients. In case which high blood sugar control is successful, microalbuminuria is also decreased.[6]

The standard method for detection of microalbuminuria is radioimmunoassay method. But due to the fact that this method is difficult to perform and have to expose to radioactive substance, therefore, the immunoturbidimetric method for determination of microalbuminuria is introduced. Not only efficacy of these diagnostic tests but also economical aspects of them should be considered. This study was set to analyze cost-effectiveness of the laboratory tests for the determination of microalbuminuria. The result from this study can be a guideline and help the physician to select the proper and economical method for the detection for microalbuminuria.

MATERIALS AND METHODS

Data about cost and effectiveness of two laboratory diagnostic tests for microalbuminuria; radioimmunoassay and immunoturbidimetric tests were reviewed. Cost in this study was set as customer cost of financial unit and presented in baht. Prevalence of disease detected in popula-

[1] Department of Laboratory Medicine, Faculty of Medicine, Chulalongkorn Univeristy

tion from the previous study[7] was set as utility. Results from each category were collected and analyzed using economical statistical method. The probabilities for each mathods were determined from the test characteristics derived from our previous validation studies.[7] The expected cost of each strategy was derived by multiplying the cost for each method with the probability of that method and subsequently adding all such products derived from the methods of that strategy. Similarity of the expected utility of each strategy was determined.

RESULTS

Customer cost and utility of each diagnostic method was shown in Table 1. Expected cost and utility of each method and cost - effectiveness of each method was presented in Table 2. The results have shown that immunoturbidimetric is more cost-effective method than radioimmunoassay in the detection for microalbuminuria (Figure 1).

Table 1. Costs and utilities of diagnostic methods for microalbuminuria.

Methods	result	Path probabilities	Customer costs (baht)	Utilities (rate)
Radioimmunoassay	+	0.33	150	0.33
	-	0.67	150	0.67
Immunoturbidimetric	+	0.14	50	0.33
	-	0.86	50	0.67

Table 2. Cost-effectiveness analysis.

Strategies	Expected cost	Expected utility	Cost-effectiveness*
Radioimmunoassay	150	0.56	267.86
Immunoturbidimetric	50	0.62	80.65

* cost effectiveness = expected cost/ expected utility

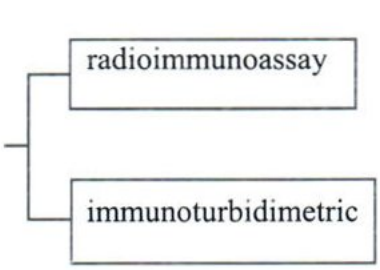

	results	probabilities	costs	utilities
radioimmunoassay	+	0.46	150	0.33
	-	0.54	50	0.67
immunoturbidimetric	+	0.46	50	0.33
	-	0.54	50	0.67

Fig. 1. Decision tree depicting laboratory diagnostic tests for microalbuminuria strategies and associated probabilities, costs and utilities.

DISCUSSION

Slight albuminuria or microalbuminuria, defined as an albumin concentration above normal but still negative by conventional dipstix testing, has recently been recognized as an early marker for diabetic complications especially for diabetic nephropathy.[2-3] In type 2, non - insulin - dependant diabetic patients, microalbuminuria can also serve as an indicator of early death from cardiovascular diseases.[1] Therefore, identification of microalbuminuria in diabetic patients implies a benifit for diabetic care.

There are many methods for determining microalbuminuria. RIA is a widely used quantitative method for microalbuminuria detection. Some limitations of this method such as, long time required for turn-over and its radiation hazard should also be considered. Therefore, an alternative methods using immunoturbidimetric test for detection of microalbuminuria have been developed.

Therefore, there are many tests for detection of microalbuminuria used in the present day. Each method has its specific property and different from the others. Checking for its efficacy and cost-effectiveness should be performed. Furthermore, in the present day, the concept of health economics was widely discussed. Each laboratory test should be check for its economical effectiveness. Therefore, this study can be a good basic information for the selection of a diagnostic test for microalbuminuria.

In this study, two common diagnostic methods for detection screening of microalbuminuria were evaluated. It was shown that the expected cost of immunoturbidimetric determination was lower than that of the radioimmunoassay test. Furthermore, the expected utilities of the immunoturbidimetric test was also higher than radioimmunoassay test. Therefore, the study revealed that immunoturbidimetric was more cost-effective method. Therefore, the selection to use this determination as a diagnostic test for microalbuminuria is rational.

This study has taken the cost for the test which the patient has to pay each test, so the cost-effectiveness analysis in this study will affcet on the patient directly.

This study has done at only one hospital and the capital investment for the laboratory, the building, the apparation and the salary of the technicians, etc. were not taken into account. Therefore, further study as a multi centric setting is recommended.

This study made use of customer cost that patient had to pay for the test in analysis so the cost-effectiveness analysis in this study can be indicated the real effect to the patient who was the customers. Based on the principle that patient should get the most cost-effective laboratory test, therefore, cost-effectiveness analysis of present laboratory service should be studied.

This study did not use total laboratory cost, which consists of direct and indirect cost and is difficult to find and the setting is limited at only one hospital. Therefore, further study as a multi center setting is recommended.

REFERENCES

1. Mattock MB, Morrish NJ, Viberti GC, Keen H, Fitzgerald AP, Jackson G. Prospective study of microalbuminuria as predictor of mortality in NIDDM. Diabetes 1992;41:736 - 41
2. Viberti GC, Hill RD, Jarett RJ, Argyropoulos A, Mahmud U, Keen H. Microalbuminuria as a predictor of clinical nephropathy in insulin-dependent diabetes mellitus. Lancet 1982;1:1430-2
3. Matheisen ER, Oxenboll B, Johansen K, Svendsen PA, DEckert T. Incipient nephropathy in type 1 (insulin-dependent) diabetes. Diabetelogia 1984;26:406-10
4. Mogensen CE, Christensen CK. Predicting diabetic nephropathy in insulin-dependent patients. N Eng J Med 1984;311:89-93
5. Mogensen CE. Microalbuminuria predicts clinical proteinuria and early mortality in mautrity of onset diabetes. N Eng J Med 1984;310:356-60
6. Feldt-Rasmussen B, Mathiesen ER, Deckert T. Effect of two years of strict metabolic control on progression of incipient nephropathy in insulin-dependent diabetes. Lancet 1986;2:1300-4
7. Ujjin P, Wiwanitkit V, Srijindaratana S. Evaluation of Microalb immunoturbidimetric test for albuminuria screening. Asian Pac J Allergy Immunol 2000 Jun; 18:177-80

A MICROCOMPUTER BASED DIGITAL RADIOTHERAPY SIMULATOR AT CHULALONGKORN UNIVERSITY

Chonlakiet KHORPRASERT MD., Chotika JUMPANGERN Msc., Chulee CHAROONSANTIKUL Bsc.

ABSTRACT

To enhance quality and readiness of radiotherapy simulation at division of radiation oncology, Chulalongkorn University, we have assembled an in-house microcomputer based digital radiotherapy simulator, which consists of a conventional simulator, analog to digital video converter, microcomputer, laser printer and image processing and archiving software. We selected Scion Image for Windows as an image processing and archiving software. Scion Image for Windows is the Windows version of Scion Image, which is in turn a version of the popular Macintosh program, NIH Image, written at the US. National Institutes of Health. Scion Image may be used to capture, display, analyze, enhance, measure, annotate, and output images. The high-resolution digital images are processed and displayed in about 1 sec, as opposed to a minimum of approximately 15-min for film. The images have been captured and stored in a server computer, so they can be easily reviewed and reprinted from any computer in our division. Because of the advantages of short image acquisition and display times, they were observed in all cases, so this system reduces radiation exposure to the patients.

INTRODUCTION

Traditional film screen imaging is more and more being replaced by digital imaging using various technologies in converting traditional images into digital images. Digital imaging offers various new possibilities in image processing, storage and transmission. This may yield additional diagnostic information, dose reduction and fast availability of images. Images will be taken without film cassettes and will be directly displayed on monitors for reporting. Digital imaging provides greater flexibility in processing, transmitting and displaying images. It is powerful and relatively inexpensive, microcomputers have been available for many years. With the development of icon-based windowing operating systems and hardware optimized for graphics, they have enable us to assemble the low cost digital radiotherapy simulator. We describe a microcomputer based digital radiotherapy simulator, which consists of a conventional simulator, analog to digital video converter and image processing and archiving software. This low cost system is designed to produce digital simulation images from radiotherapy simulator. The system is based upon a standard microcomputer and operates using the simulator's image intensifier as the source of video signal for analog to digital video converter.

Division of Radiation Oncology, Department of Radiology, Faculty of Medicine, Chulalongkorn University, Bangkok.

MATERIAL AND METHOD

Hardware

1. Conventional simulator.
2. ASUS® V3800 TVR display card, which can convert analog video signal to digital video signal.
3. A personal computer bases upon Intel Pentium processor series with network capability.
4. Local area network.
5. Laser image printer.

Our simulator is Ximatron CX simulator from Varian Medical System,Inc.. It is a conventional simulator with fluoroscopy. It includes a built-in charged-couple (CCD) device camera, which views the x-ray image optically transmitted from a conventional phosphor screen. The image is sent to a monitor for on-line viewing. After proper simulation image is seen on a monitor, a hard copy image on photographic film is produced for every patient. To convert analog video signal to digital form, the video signal of simulation image is diverted to ASUS® V3800 TVR display card within a personal microcomputer from fluoroscopic monitor (Fig.1). The computer is one of the computers in radiation oncology network at King Chulalongkorn Memorial Hospital.

Software

1. Microsoft® Window 95.
2. ASUS® live video captures software.
3. Scion Image for Windows.

We chose ASUS® live video capture driver and Scion Image for Windows as a digital video capture software and image processing software respectively. They need Microsoft® Window 95 to be operated. Microsoft® Window 95 is operating system that is widely used and consists of many powerful tools. The ASUS® live video capture driver follows Microsoft Video for Windows standard and can open up to a capture window size of 704 x 480 pixels, 30 frames/second. Video Snapshot function of the driver lets us capture video stream data as single images and then show these images on desktop almost simultaneously through the image viewer selected. It supports any plug-in image-processing program, Scion Image for Windows. Scion Image for Windows is the Windows version of Scion Image, which is in turn a version of the popular Macintosh program, NIH Image, written at the National Institutes of Health. Scion Image may be used to capture, display, analyze, enhance, measure, annotate, and output images. Scion Image extensively supports all Scion frame grabber boards, and provides a powerful and complete image acquisition environment. Scion Image for Windows supports color and grayscale image capture with Scion frame grabbers. It includes advanced capturing capabilities such as frame averaging and summation, frame sequence capture, and on-chip integration support. All current features of NIH Image have been included.[1] This program is available free of charge. Scion provides full technical support to users of Scion Image.

RESULTS AND DISCUSSION

The high-resolution digital images are processed and displayed in about 1 sec, as opposed to a minimum of approximately 15-min for film In fact, we do not have film-processing unit in our division. Digital images of various radiation fields have been done with good resolution. Figures 2-4 show different sites of treatment fields.

These digital radiographs provided permanent high-resolution images as required in most cases for verification of treatment fields. All of the images have been stored in our division server computer, and Scion Image for Windows can be

installed on any remote computer in the computer network, so the physicians can access and review the images from any computers in the division. Apart from acquiring and displaying the images, Scion Image can edit, enhance, analyze and animate images. It reads and writes TIFF, PICT, PICS and MacPaint files, providing compatibility with many other applications, including programs for scanning, processing, editing, publishing and analyzing images. It supports many standard image processing functions, including contrast enhancement, density profiling, smoothing, sharpening, edge detection, median filtering, and spatial convolution with user defined kernels which found to be very useful for image enhancement. Scion Image can be used to measure area, mean, centroid, perimeter, etc. of user defined regions of interest. It also performs automated particle analysis and provides tools for measuring path lengths and angles. Spatial calibration is supported to provide real world area and length measurements. Density calibration can be done against radiation or optical density standards using user-specified units. Results can be printed, exported to text files, or copied to the Clipboard. A tool palette supports editing of color and gray scale images, including the ability to draw lines, rectangles and text. It can flip, rotate, invert and scale selections. It supports multiple windows and 8 levels of magnification. All editing, filtering, and measurement functions operate at any level of magnification and are undoable. Many features of Scion Image were found to be very useful for imaging in regions of different density, such as lung and soft tissue, in the same radiograph.

There are some limitations of this approach. First, the quality of image is influenced by many factors such as quality of simulator's phosphor screen and CCD device camera that produce analog video image, display card resolution and laser printer quality. Second, there are some distortions of the images that may cause by CCD camera. Straight line is not exactly straight. It is slightly curved. Third, the maximum field size is about 16 by 16 centimeters that is the maximum field of view of CCD camera. If we need simulation images with radiation portal more than 16 by 16 centimeters we have to take more than one image at different ends of portal, so the physicians could see all of the boundaries of the portal. (Figure 5)

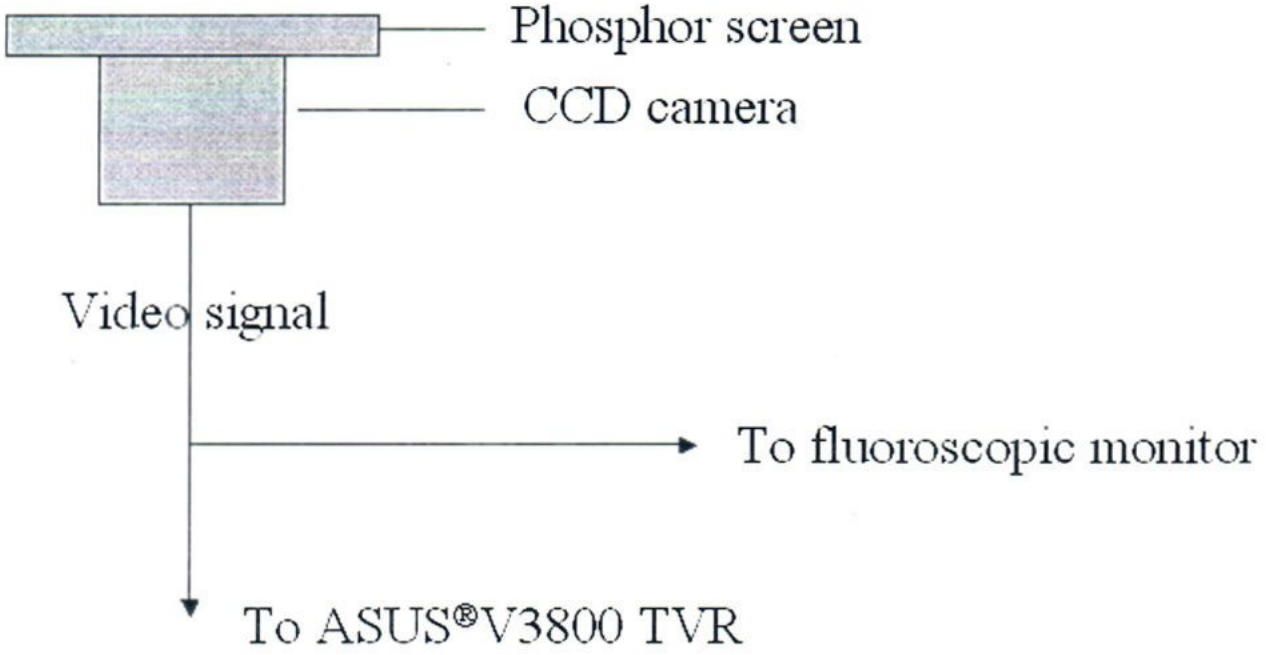

Fig.1 Diverting of analog video signal from CCD camera to ASUS® V3800 TVR

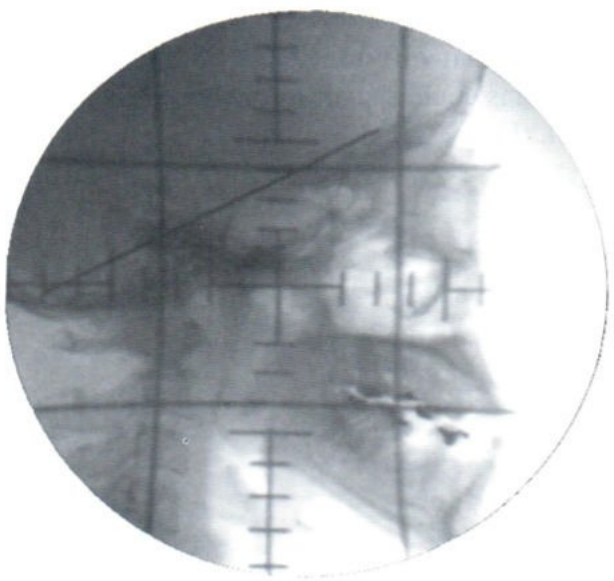

Fig. 2 Radiation portal at nasopharynx.

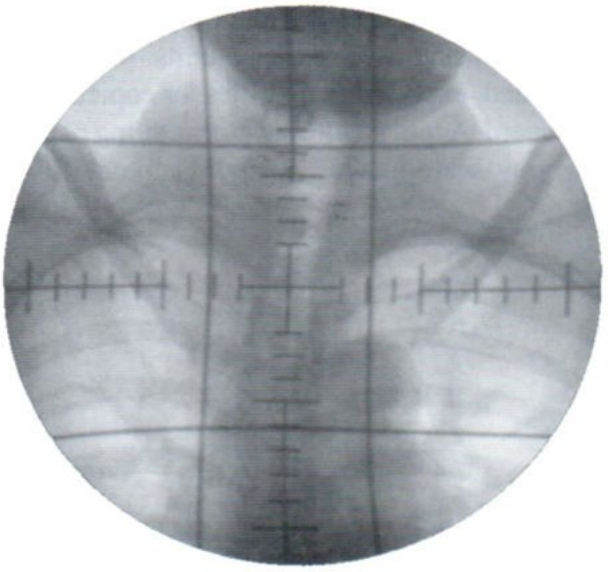

Fig. 3 Radiation portal at thoracic area.

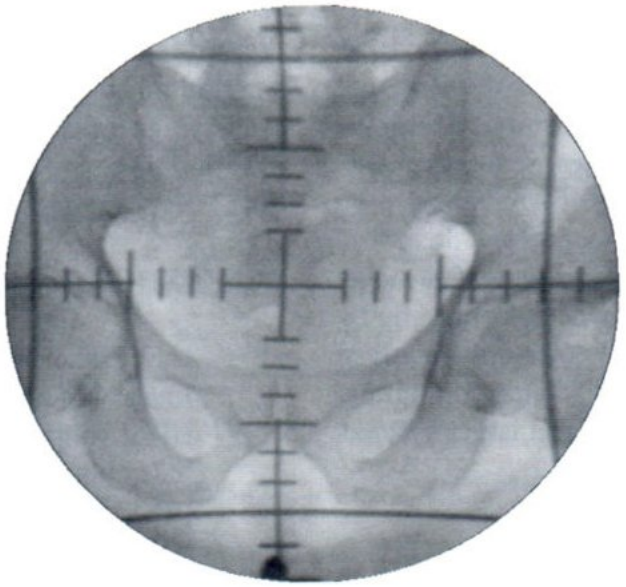

Fig. 4 Radiation portal at pelvis.

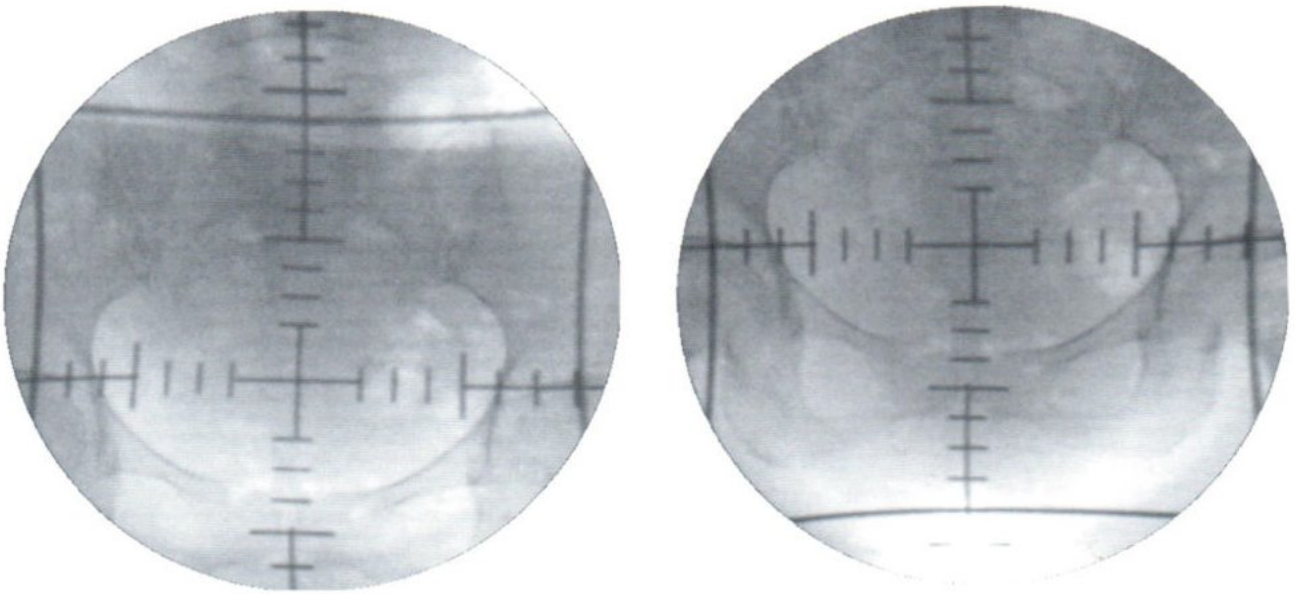

Fig. 5 Image at upper end (right) and lower end (left) of radiation field.

Because it require only 1 second per image for processing and displaying, the advantages of short image acquisition and display times were observed in all cases. So this approach also enables a new method of simulation to be considered which reduces patient dose and prolongs the useful working life of the X-ray tube. However, this trend is influenced technically by the advent of more efficient detectors, improved image processing methods, faster computers, brighter and sharper displays and larger systems for image storage and archiving.

CONCLUSION

A microcomputer based digital radio-therapy simulator enables a new method of simulation, which enables fast image display processing; archiving and reduction of patient radiation dose and prolongs the useful working life of the X-ray tube.

REFERENCE

1. U.S. National Institutes of Health . NIH Image Manual (V1.61). Available from: URL: http://rsb.info.nih.gov/nih-image/index.html